

We are IntechOpen, the world's leading publisher of Open Access books Built by scientists, for scientists

6,900

Open access books available

186,000

International authors and editors

200M

Downloads

Our authors are among the

154

Countries delivered to

TOP 1%

most cited scientists

12.2%

Contributors from top 500 universities



WEB OF SCIENCE™

Selection of our books indexed in the Book Citation Index
in Web of Science™ Core Collection (BKCI)

Interested in publishing with us?
Contact book.department@intechopen.com

Numbers displayed above are based on latest data collected.
For more information visit www.intechopen.com



Finite element analysis on strains of viscoelastic human skull and duramater

Xianfang YUE*, Li WANG, Ruonan WANG and Feng ZHOU
*Mechanical Engineering School,
University of Science and Technology Beijing, Beijing 100083
China*

1. Fundamental Theory of Finite Element

There are many mechanics and field problems in the domain of engineering technology, such as the analyses of stress-strain field, displacement field, temperature field in the heat conduction, flow field in the hydrodynamics, electromagnetic field in the electromagnetism, etc, which can be considered as the problems to solve the basic differential equations with a certain boundary conditions. Although the basic equations and boundary conditions have been established, very few simple questions can be solved to obtain the analytical solution. For the questions with complex mathematical equations or irregular physical boundary, it is insurmountably difficult to solve the mathematical problems by analytical method. There are usually two ways to solve such problems: one is the analytic method, another is the numerical method. After introducing the simplifying assumptions, the analytic method can be used to get the approximate solution. But this approach is not always feasible to the actual problems, so the incorrect or wrong answers will always be led to. To meet the needs of the complex project problems, the numerical solution can be adopted to finish a variety of effective numerical calculation. At present, numerical solution methods in engineering practical applications commonly include the limited element method, finite difference method, the boundary element method, weighted residual method, etc. With the rapid development and extensive application of computer, the finite element method, a relatively new and very effective numerical method, has gradually been used to solve the complex engineering problems.

1.1 Finite Element Method, FEM

Finite Element Method (FEM) is an integrated product of many disciplines, including mechanics, mathematical physics, computational methods, computer technology, and so on. The three research methods, theoretical analysis, scientific experiments and scientific

* Corresponding author. Address: School of Mechanical Engineering, University of Science and Technology Beijing, Beijing 100083, China

Tel.: +86-01-62332743; Fax: +86-10-62332743.

E-mail address: yuexf@me.ustb.edu.cn

computing, have been applied to study the nature problems. Because of the limitations of scientific theory and experiments, the scientific computing becomes one of the most important research tools. As one of ways to carry out the scientific computing, the finite-element method can almost analyze any complex engineering structure so as to obtain various mechanical properties in most engineering fields.

The analyses of various mechanical problems can be concluded to the following two forms : the analytical method and the numeric method. If a problem given, the answers can be got by some derivation, which is called the analytical method. Due to the complexity of the actual structure, it is difficult to analytically solve the majority of scientific researches and engineering problems except for a few very simple questions. Therefore, the numerical methods, such as the finite element method, finite difference method, boundary element method, have become the irreplaceable and widely used methods. Rrapidly developed in the mid-20th century, the finite-element method can flexibly analyze and solve various complex problems for the precise mathematical logic, clear physical concept and wide utilization. By adopting the matrix, the finite-element method can conveniently make computer programs to express the basic formula, which makes it vitality.

The essence of the finite-element method is that a complex continuum is divided into a limited number of simple cell body, which transforms the infinite freedom degrees to the limited freedom degree, and the (partial) differential equation to the algebraic equations of finite number of parameters. While analyzing the problems of engineering structure with the finite-element method, after the discretization of an ideal discrete body, it is one of main discussing contents of the finite-element theory how to ensure the convergence and stability of numerical solution. The convergence of numerical solution is related to the element division and shape. During the solving process, as the basic variable, the displacement is usually solved through the virtual displacement or minimum potential energy principle.

The finite-element method is initially applied in the fields of engineering science and technology. As a mathematical and physical method, the finite-element method is used to simulate and solve the problems of engineering mechanics, thermology, electromagnetism and other physical subjects. Moreover, as a numerical analytical method with theoretical foundation and extensive applicable effect, it can solve the problems can't be dealt with by the analytic method. Especially for the complex issues of the irregular boundary conditions or structural shapes, the finite-element method is an effective modern analytical tool. In recent years, the application and development of the finite-element method in the field of bio-mechanics show as follows:

1.1.1 Generation of the Finite-element method

The basic ideas of the finite-element method are usually regarded to begin in the 20th century. In fact, as early as the 3rd century AD, it is the basic expression when Hui Liu, a Chinese mathematician, suggested the method to solve the circumference length by the segmentation unit. According to the thought solving the internal force of structural frame in the classical mechanics, the structural frame is treated as the finite pole elements connected at the junction points in the displacement method, in which each pole element is firstly studied and then finally comprehensively analyze the combination of pole elements. The basic idea of finite-element method is early discretization and later integration.

In 1942, Hrenikoff first proposed the framework method solving mechanical problems, which is only limited to construct the discrete model with the plot series of structure. In 1943,

Courant [1] published a paper to solve the reverse problem by using the polynomial function in the triangular region, in which the flexure function is originally assumed as a simple linear function on each element in a collection of triangular element collection. It is the first time to deal with the continuum problem by the finite element method.

In 1950', due to the rapid development of aviation industry, more accurate design and calculation needed be used in the aircraft structure. In 1955, the professor JH Argyris in the University of Stuttgart, Germany, published a set of papers about energy principles and matrix, which laid the theoretical basis of the finite element method. In 1956, Turner, Clough, Martin, Top, etc, extended the displacement method to the plane problems of elasticity, and use it in the aircraft structural analysis and design. By systematically study the stiffness expression of discrete bar, beam, triangular elements, the correct answers are be obtained for the plane stress problems. Thus their work began the new phase to solve complex elasticity problems using computers.

In 1960, Clough firstly proposed and used the name of "finite element method" while dealing with the section elastic problems, which made people better understand the characteristics and effectiveness of this approach. Since then, a large number of scholars and experts begun to use the discrete approach to deal with the complex issues of structural analysis, fluid analysis, thermal conductivity, electromagnetism, etc. From 1963 to 1964, Besseling, Pian T.H. and other researchers proved that the finite-element method is actually one of means of Rayleigh - Ritz method in the elasticity variational principles, which in theory lays a mathematical foundation for the finite-element method. Compared with the variational principle, the finite-element method is more flexible, adaptable and precise. The results also greatly promoted the research and development of variational principle, and a series of new finite-element models have been emerged based on the variational principle, such as the mixed finite element, non-conforming element, generalized conforming element, etc. In 1967, Zienkiewicz and Cheung published the first book on the finite-element analysis. After the 1970', the finite-element method entered into high-speed period with the development of computer technology and software technology. At that time, the in-depth research was carried out on the finite element method, including the theories in the fields of mathematics and mechanics, principles of element division, the selection of shape functions, numerical methods, error analysis, convergence, stability, computer software development, nonlinear problems, large deformation problems, etc. In 1972, Oden published his first book dealing with non-linear continuum. In the process of development of finite-element method, chinese scientists have also made the outstanding contributions, for example the generalized variational principle proposed by Changhai Hu, the relationship between Lagrange multiplier method and generalized variational principles first studied by Weichang Qian, the accuracy and convergence of finite element method made by Kang Feng, the complementary energy principle by Lingxi Qian, and so on.

With the continuous development and improvement, the finite-element method has become a mature discipline, has been extended to other research fields, and become a powerful tool to solve practical problems for the science and technology researchers.

1.1.2 Basic Theory of the Finite-element method

The finite-element method is a general numerical one dealing with continuum problems. The basic idea of finite-element method is to split up, and then accumulate zero into the whole, which is artificially divided a continuum into finite elements. That is, a structure is

regarded as an integral made up of elements joined by the number of nodes. After the element analyses, the assembled elements are overall analyzed to represent the original structure. From the view of mathematical point, the finite element method is one that turns a partial differential equation into an algebraic equation, and then solved by computer. Using a matrix algorithm, the results can be quickly calculated through the computer.

The basic theory of finite element method is firstly to discretize the continuous computational region into a finite number of unit integration linked together by a certain forms. As the unit can be combined by different connected ways and the unit itself can have different shapes, it can be simulated to solving small region of different geometric shapes, then the units (small area) are carried out on the mechanical analysis, and finally is the overall analysis. That is the basic idea which breaks up the whole into parts and collect parts for the whole. Another important feature of the finite-element method is to express piecewise the unknown field function in the sub-domains by using the hypothetical approximate function in each unit. The approximate function is usually expressed by unknown field function or the data and difference of derivative on each node. Thus, the unknown field function or derivative in each node become the new unknown amounts (the degrees of freedom) while analyzing the problems using the finite-element analysis. So that the issues of continuous unlimited freedom become those of the discrete limited freedom. After solving these unknown variables, the approximation of field function in each element can be calculated by interpolation, and then the approximate solution can be obtained in the entire solution region. With the increasing unit numbers (decreasing unit size), or with the rising element freedom degree and improved accuracy of interpolation function, the solutions approximation is continuously improved. As long as each unit meets the convergence requirements, the approximate solution will eventually converge to the exact solutions.

1.1.3 The characteristics of finite-element method

(1) The adaptability for complex geometry components

As the finite element method of cell division can be one-dimensional, two-dimensional, three-dimensional in space, and can have different shapes, such as two-dimensional elements can be triangular, quadrilateral, 3D element can be tetrahedral, five-sided, six sided, etc. At the same time, the modules can also have different connection forms. Therefore, any complex structure or construction in the practical application can all be separated into a collection made up of finite of modules.

(2) The adaptability for a variety of configuration problems

The finite element method has been developed from the first pole structure to the current plastic, viscoelastic-plastic and power issues of problems, which can be used to solve various complex non-linear problems in the fluid mechanics, thermodynamics, electromagnetism, aerodynamics.

(3) The reliability of theoretical basis

The theory of finite element method is based on variational and energy-conservation principles, which have been reliably proven in mathematics and physics. As soon as the mathematical model is appropriately set up and the algorithm of finite element equation is stable convergence, the solution obtained are authentic.

(4) The credibility of accuracy

As long as the research question itself is solvable, the accuracy of finite element method will

be continually increased as the cell number increases in the same conditions, then the approximate solutions will keep close to the exact ones.

(5) The efficiency of calculation

As each step of the finite-element analysis can be expressed in matrix form, the final solutions come down to solve the standard matrix algebra problem, which particularly suitable for computer programming calculations by turning a number of complex differential, partial differential equations into solving algebraic equations.

1.2 The analysis process of finite-element method

1.2.1 The discretization of structure

The first step of a finite element analysis is to decentralize the structure, that is, to divide the entire structure into a finite element based on different accuracy requirements, performance requirements and other factors. The positions between elements or element and boundary are connected by nodes.

During the discretization, we must pay more attention on the following three points: the choice of element types, including element shape, node number, and node number of freedom, a certain regularity of element partition, in order to compute the network of automatic generation, and then conducive to encrypt the network. And the same element should be composed of the same material.

1.2.2 The element analysis

The element analysis regards each discretized element as a research object. The relationship between node displacement and the nodal force includes the following two aspects:

(1) Determine the displacement mode of element

For the displacement finite-element method, the displacement model of element is to calculate the displacement at any point with the node displacement of element, in which the element displacement can be expressed as a function of node displacement. It directly affects the accuracy, efficiency and reliability of finite element analysis whether or not a reasonable assumption of displacement function.

(2) Analyze the element characteristics

After establishing the displacement function of element, according to the relationship among stress, strain and displacement, the relationship between the element rod end force and displacement of rod end and then the element stiffness matrix are obtained by using the virtual displacement and minimum potential energy principles. Here the load on the element must be equivalent to the node load. Thus the element analysis is in fact the process to set up the element stiffness and equivalent nodal load matrixes.

1.2.3 The overall analysis

After determining the stiffness equation of each element, you can set the various units of a whole structure, the node balance equations of entire structure are established, that is the overall stiffness equation, through analyzing the whole structure gathered by each element. After the introduction of structural boundary conditions, the equations are solved to reach the node displacement, and then the internal force and deformation of each element.

1.3 Steps to solve the finite element method

When any continuum are solved with the finite element method, the solution continuous

area should be divided into a finite number of elements, and a finite number of nodes are specified in each element. Generally, the adjacent elements can be considered to constitute a group of element by in the nodes, and then form the collection which is used to simulate or approximate the solving region. At the same time, the node data are selected in the field function, such as the node displacement regarded as the basic unknown quantity. By the block approximation to each element, a simple function (called interpolation function) can approximately express the assuming the displacement distribution. Using the variational principle or other methods, a set of algebraic equations can be obtained in which the nodal displacements is regarded as the unknowns by establishing the mechanical properties relationship between force and displacement of element nodes. Thereby the node displacement components can be solved. The approximate function in the element is usually expressed by the unknown field function or each node data of field functions and their interpolation function. Thus, in the finite element analysis, the unknown field function or derivative values of each node in the element becomes a new unknown quantity (ie degrees of freedom). Then a continuous problem of infinite freedom degrees becomes the discretized problem of limited freedom degrees. Upon solving these unknowns, the approximation of field function in each element can be calculated by interpolation function, and the approximate solution in the overall solving domain can be obtained. Obviously, if the element meet the convergence demands of problem, the approximate level of solution will be improved with the shrinking element size, increasing element numbers in the solving region, rising element freedom degree or improving accuracy of interpolation function, and finally the approximate solution will eventually converge to exact solutions.

While solving the mechanics problems by using the finite element method, the basic unknowns mustn't be given with the node displacement but the node force. Therefore, for the different taken basic unknown quantity, there are the so-called displacement, hybridization and mixing method, in which the displacement method is the most common. The ANSYS, well-known large-scale commercial software, adopts the finite element displacement method [2,3].

1.4 The basic steps of the finite element method [4]

(1) Discretization of objects and selected element type

The core of the finite element method is discretization. For each specific issue, the specific content of discretization is how to choose the appropriate element type to determine element size, number, layout and sequential manner of nodes. Element size is small enough to ensure the accuracy of calculation, and element size is large enough to reduce the computation workload. In theory, the finer elements, the more nodes can be arranged, and more accurate the results are. Today, the computer's capacity and speed are not the principal contradiction. However, it shows that the grid encrypt is not effective for improving the calculation accuracy after the numbers of nodes and elements reach a certain value. The general principle divided into elements: the element nodes should be those of intersection, turning, support and sectional mutations points in the structure.

(2) The analysis of element

The element analysis is to solve the relationship between the nodal displacement of basic unknown quantity and the corresponding nodal forces. For the element, the Nodal forces are the external forces on the elements through the nodes, which determines not only the displacement of this node, but also the effects of other nodes in this element. After

determining the element displacement, the stress and strain of elements can be easily obtained by the geometric and physical equations. In general, the stiffness matrix can express the element properties, and then the relationship between the element nodal force and displacement can be determined.

(3) The overall analysis

The overall analyses include the combination of whole stiffness matrix and the establishment of balance equations. The whole stiffness matrix is made up of the element stiffness matrix, and each item contains all corresponding information of relevant elements of nodes.

(4) The introduction of support conditions and total load of nodes

The support conditions are constraint ones. Suspended structures without constraint can't support the loads. The total loads of nodes include ones acted on nodes and the non-node ones of equivalent transplant. The node load vectors are consistent with node force vectors of overall stiffness equations. After changing the node force vector of overall stiffness equations to the node load vectors, the node balance equations are established and the nodal displacements as unknowns.

(5) The nodal displacement by solving the finite-element equations

All unknown nodal displacements can be solved for solving algebraic equations with the finite-element software.

(6) Return to the results of element calculation

The element strain can be solved by the nodal displacements, and the element stress can be reversed through the physical equations.

1.5 The finite-element method is the synthesis of a variety of methods [4]

At first, the finite element method is a kind of model one. The model is a kind of simplified description on a simplified understanding of the objects' for a particular purpose. By studying the prototype model, it reveals the morphology, characteristics and nature of objects. An important feature of the finite element method is to express the unknown function to be calculated in the overall solution domain by using the approximate function supposed in each element. Then there is an approximation problem between approximate and real solutions. Obviously, the approximation degree of solution is higher with the increasing element numbers, that is the shrinking element size, or with the rising element freedom degree, that is the improved interpolation function. Secondly, the finite-element method is the result about the integrated application of the analysis and comprehensive methods. The first part work of finite-element method is to discretize the study object into many simple shapes and easy description. According to the special circumstances, the object can be discreted to the two-dimensional or three-dimensional finite element collections, in which the discreted elements have simple and regular geometry easy to calculate. For the two-dimensional elements, there are normally triangular or rectangular. For three-dimensional elements, there are commonly tetrahedral or parallelepiped. For the same shape of element, there are different nodes, so many different kinds of elements. According to various analysis object and purpose, the elements selected are different.

1.6 The application of finite-element method in bio-mechanics

It has made great achievements that the finite-element method is applied the life science to carry out the quantitative research. In particular, its great superiority is demonstrated in the

research on human biomechanics. After a long evolution of human labor, the human skeleton has almost formed a perfect mechanical structure. However, the mechanics experiment is almost impossible to directly develop while the mechanical structure of human body is studied. At that time, it is an effective means that the finite element numerically simulates the mechanical experiments.

In 1960's, the finite element method was initially applied in the cardiovascular system study on mechanical problems. From the 1970's, the orthopedic biomechanics research began to be initially applied to spine. After 80 years, the applicable range is gradually extended to craniofacial bone, mandible bone, femur[5], teeth[6], joint[7, 8], cervical [9], lumbar [10] and its subsidiary structure in the bio-mechanics fields.

(1) Improvement and optimization design of equipment

The finite element analysis can improve the mechanical properties of medical devices and optimize the design of equipment. The mechanical properties of medical equipment often determine the effectiveness of the clinical application. Therefore it is more important to evaluate the mechanical properties of appraisal instrument. In addition to the experimental methods, the simulative experiment to the mechanical equipment with the finite-element method has the advantages of short time, cost less, handling complex conditions, comprehensive mechanical properties and good repetitiveness, etc. In addition, the finite-element method can also optimize the design, guide the design and improvement of medical devices, and obtain better clinical effects.

(2) The mechanical simulation experiment by finite element model

The powerful modeling capabilities and interface tool if the finite element software can distinctly build the models of three-dimensional human bone, muscle, blood vessels and other organs, and be able to give their biomechanical properties. In the simulated experiments, the model simulation to experimental conditions and mechanical tests to simulate the stretching, bending, torsion, anti-fatigue can solve the deformation, stress, strain distribution, the internal energy change and the ultimate destruction situation on different experimental conditions [11].

(3) Nowadays, the finite element method has been widely used in the country, and has made a lot of successes. Particularly, there are more certain guidances in the clinical application. In bio-mechanics the finite-element application, there are a large number of spaces to research the shape and structure of finite element model.

2. Mechanical Analysis of cranial cavity deformation

2.1 Mechanical Analysis of deformation of the skull as a whole

There are two aspects of effects on external forces on the objects. One can make objects produce the acceleration, another is make objects deform. In discussing the external force effect, the objects are assumed to be a rigid body not compressed. But in fact, all objects will deform under loading, but different with the degrees. Here, we will mechanically analyze the overall deformation of cranial cavity under the external force.

(1) Two basic assumptions

To simplify the analysis of deformation of human skull, we assume:

1) Uniformly-continuous materials

The human skull is presumed to be everywhere uniform, and the sclerotin is no gap in bone of cranial cavity.

2) The isotropy

The human skull is supposed to have the same mechanical properties in all directions. The thickness and curvature of human skull vary here and there. The external and internal boards are all compact bones, in which external board is thicker than internal board but the radius of external board is smaller than that of the internal board. The diploe is the cancellous bone between the external board and the internal board, which consists of the marrow and diploe vein. The parietal bone is the transversely isotropic material⁸, namely, it has the mechanical property of rotational symmetry in any axially vertical planes of skull⁹. The tensile and compressive abilities of compact bone are strong. The important mechanical characteristics of cancellous bone are viscoelasticity¹⁰, which is generally considered as the construction of semi-closed honeycomb composed of bone trabecula reticulation. The main composition of cerebral duramater, a thick and tough bilayer membrane, is collagenous fiber¹¹, which is viscoelastic material¹². And the thickness of duramater is obviously variable with the changing ICP¹³. The mechanical performance of skull is isotropic along tangential direction on the skull surface¹⁴, in which the performance of compact bone in the external board is basically the same as that in the internal board¹⁵, thus both cancellous bone and duramater can be regarded as isotropic materials¹⁶. And the elastic modulus of fresh duramater is variable with delay time¹⁷. And there are a number of sutures in the cranial cavity. But while a partial skull is studied on the local deformation, we can regard each partial skull as quasi-homogeneous and quasi-isotropic. In addition, the sutures of cranial cavity are also the continuous integration with ages.

(2) Two concepts

(1) stress (σ)

Stress is the internal force per unit area. The calculation unit is kg/cm^2 or kg/mm^2 .

2) Transverse deformation coefficient

When the objects are under tension, not only the length is drawn out from l to l_1 , but also the width is reduced from b to b_1 . This shows that there are the horizontal compressive stresses in the objects. Similarly, while the object is compressed, not only its length shortens but its width increases. It indicates that the horizontal tensile stress distributes in the objects.

The horizontal absolute deformation is noted as $\Delta b = b - b_1$, and the transverse strain is $\varepsilon_0 = \Delta b/b$.

In mechanics of materials, the transverse strain ε_0 is proportional to the longitudinal strain ε of the same material within the scope of the Hooke theorems' application. The ratio of its absolute value $\mu = |\varepsilon_0|/|\varepsilon|$ is a constant. μ is known as the coefficient of lateral deformation, or Poisson ratio. The Poisson ratio of any objects can be detected by the experiment.

While vertically compressed, the objects simultaneously have a horizontal tension. Therefore, when the head attacked in opposite directions force, the entire human skull will take place the longitudinal compression and transverse tension with the same direction of force. Then the longitudinal compressive stress and the horizontal tensile stress will be generated in the sclerotin. Thus, the stress of arbitrary section along radial direction in shell

is just equal to the tangential pulling force along direction perpendicular to the normal vertical when ICP is raised.

2.2 The finite-element analysis of strains by ignoring the viscoelasticity of cranial cavity

The geometric shape of human skull is irregular and variable with the position, age, gender and individual. So the cranial cavity system is very complex. Moreover, the cranial cavity is a kind of viscoelastic solid with large elastic modulus, and the brain tissue is also a viscoelastic fluid with great bulk modulus. It is now almost impossible to accurately analyze the brain system. Only by some simplification and assumptions, the complex issues can be made. Considering the special structure of cranial cavity composed of skull, duramater, encephalic substance, etc, here we simplify the model of cranial cavity as a regular geometry spheroid of about 200mm external diameter, which is an hollow equal-thickness thin-wall shell.

The craniospinal cavity may be considered as a balloon. For the purpose of our analysis, we adopted the model of hollow sphere. We presented the development and validation of a 3D finite-element model intended to better understand the deformation mechanisms of human skull corresponding to the ICP change. The skull is a layered sphere constructed in a specially designed form with a Tabula externa, Tabula interna, and a porous Diploe sandwiched in between. Based on the established knowledge of cranial cavity importantly composed of skull and dura mater (Fig2.1), a thin-walled structure was simulated by the composite shell elements of the finite-element software [18]. The thickness of skull is 6mm, that of duramater is 0.4mm, that of external compact bone is 2.0mm, that of cancellous bone is 2.8mm, and that of internal compact bone is 1.2mm.

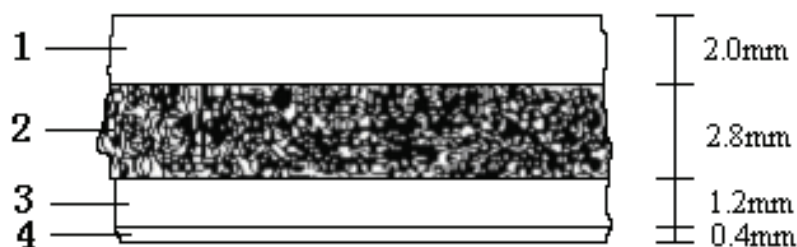


Fig. 2.1 Sketch of layered sphere. The thin-walled structure of cranial cavity is mainly composed of Tabula externa, Diploe, Tabula interna and dura mater.

Above all, we should prove the theoretical feasibility of the strain-electrometric method to monitor ICP. We simplify the theoretical calculation by ignoring the viscoelasticity of cancellous bone and dura mater. And then we make the analysis of the actual deformation of cranial cavity by considering the viscoelasticity of human skull-dura mater system with the finite-element software. At the same time, we can determine how the viscoelasticity of human skull and dura mater influences the strains of human skull respectively by ignoring and considering the viscoelasticity of human skull and dura mater.

2.2.1 The stress and strain analysis of discretized elements of cranial cavity

In order to obtain the numerical solution of the skull strain, the continuous solution region of cranial cavity divided into a finite number of elements, and a group element collection

glued on the adjacent node points. Then the large number of cohesive collection can be simulated the overall cranial cavity to carry out the strain analysis in the solving region. Based on the block approximation ideas, a simple interpolation function can approximately express the distribution law of displacement in each element. The node data of the selected field function, the relationship between the nodal force and displacement is established, and the algebraic equations of regarding the nodal displacements as unknowns can be formed, thus the nodal displacement components can be solved. Then the field function in the element collection can be determined by using the interpolation function. If the elements meet the convergence requirements, with the element numbers increase in the solving region with the shrinking element size, and the approximate solution will converge to exact solutions [12].

The solving steps for the strains of cranial cavity with the ICP changes are shown in Fig2.2. The specific numerical solution process is:

1) The discretized cranial cavity

The three-dimensional hollow sphere of cranial cavity is divided into a finite number of elements. By setting the nodes in the element body, an element collection can replace the structure of cranial cavity after the parameters of adjacent elements has a certain continuity.

2) The selection of displacement mode

To make the nodal displacement express the displacement, strain and stress of element body, the displacement distribution in the elements are assumed to be the polynomial interpolation function of coordinates. The items of polynomial number are equal to the freedom degrees number of elements, that is, the number of independent displacement of element node. The orders of polynomial contain the constant term and linear terms.

According to the selected displacement mode, the nodal displacement is derived to express the displacement relationship of any point in the elements. Its matrix form is:

$$\{f\} = [N]\{\delta\}^e \quad (2.1)$$

Where: $\{f\}$ - The displacement array of any point within the element;

$[N]$ - The shape function matrix, its elements is a function of location coordinates;

$\{\delta\}^e$ - The nodal displacement array of element.

The block approximation is adopted to solve the displacement of cranial cavity in the entire solving region, and an approximate displacement function is selected in an element, where need only consider the continuity of displacement between elements, not the boundary conditions of displacement. Considering the special material properties of the middle cancellous and duramater, the approximate displacement function can adopt the piecewise function.

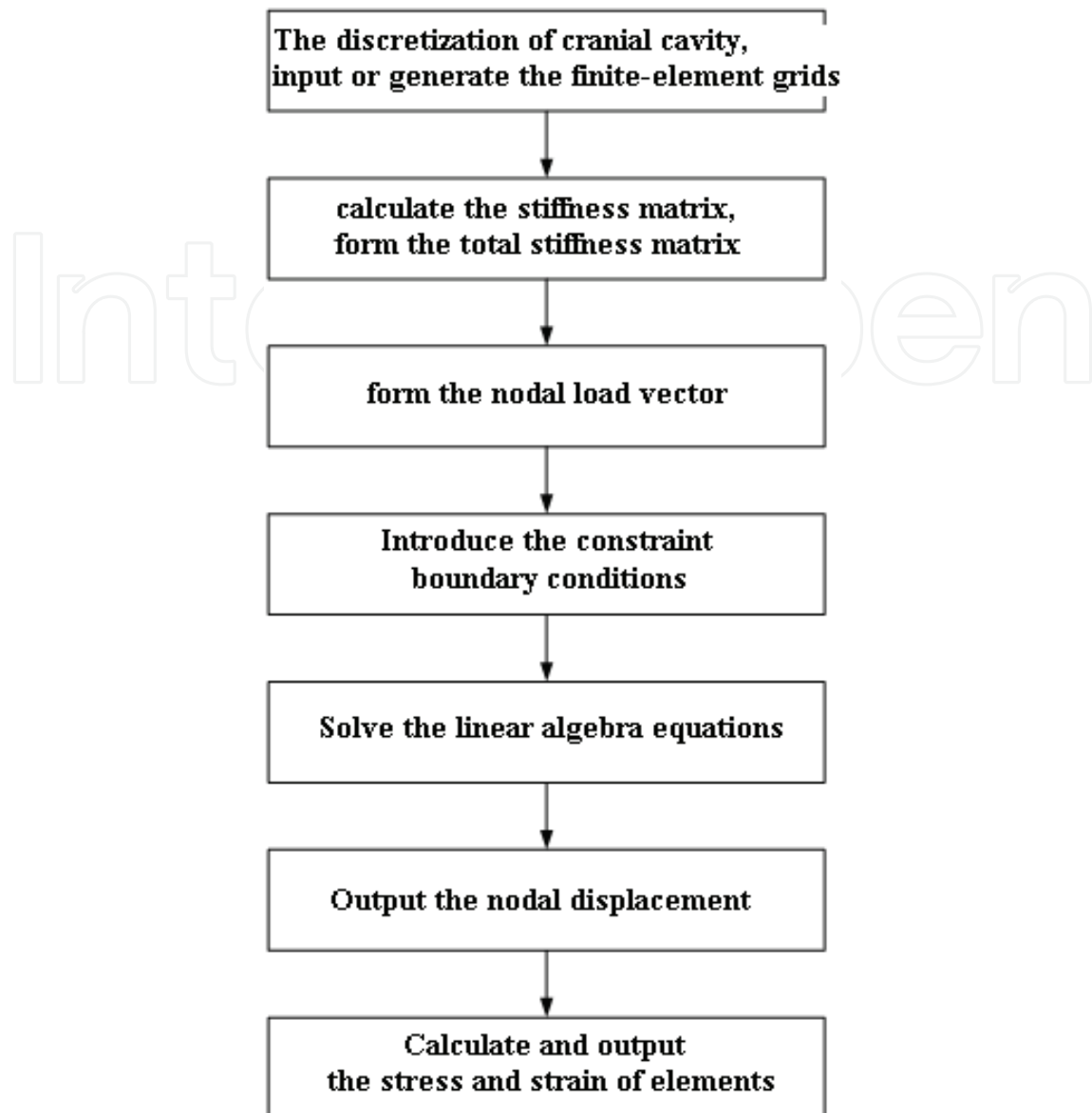


Fig. 2.2 Block diagram of numerical solution steps of cranial cavity with the finite-element method

- 3) Analyze the mechanical properties of elements, and derive the element stiffness matrix
 a. Using the following strain equations, the relationship of element strain (2.2) is expressed by the nodal displacements derived from the displacement equation (2.1):

$$\text{Strain equations} \left\{ \begin{array}{l} \varepsilon_x = \frac{\partial u}{\partial x}, \gamma_{xy} = \frac{\partial u}{\partial y} + \frac{\partial v}{\partial x} \\ \varepsilon_y = \frac{\partial u}{\partial y}, \gamma_{yz} = \frac{\partial u}{\partial z} + \frac{\partial w}{\partial y} \\ \varepsilon_z = \frac{\partial u}{\partial z}, \gamma_{zx} = \frac{\partial u}{\partial x} + \frac{\partial v}{\partial z} \end{array} \right.$$

$$\{\varepsilon\} = [B]\{\delta\}^e \quad (2.2)$$

Where : [B]—The strain matrix of elements ;

$\{\varepsilon\}$ —The strain array at any points within the elements.

b. The constitutive equation reflecting the physical characteristics of material is $\{\sigma\} = [D]\{\varepsilon\}$, so the stress relationship of stress can be expressed with the nodal displacements derived from the strain formula (2.2):

$$\{\sigma\} = [D][B]\{\delta\}^e \quad (2.3)$$

Where: $\{\sigma\}$ - The stress array of any points in the elements;

[D]- The elastic matrix related to the element material.

c. Using the variational principle, the relationship between force and displacement of the element nodes is established:

$$\{F\}^e = [k]^e \{\delta\}^e \quad (2.4)$$

Where: $[k]^e$ - Element stiffness matrix, $[k]^e = \iiint [B]^T [D] [B] dx dy dz$;

$\{F\}^e$ - Equivalent nodal force array, $\{F\}^e = \{F_V\}^e + \{F_S\}^e + \{F_C\}^e$;

$\{F_V\}^e$ - Equivalent nodal force on the nodes transplanted from the element volume

force P_V , $\{F_V\}^e = \iiint_V [N]^T \{P_V\} dV$;

$\{F_S\}^e$ - Equivalent nodal force on the nodes transplanted from the element surface

force, $\{F_A\}^e = \iint_A [N]^T \{P_S\} dA$;

$\{F_C\}^e$ - Concentration force of nodes.

4) Collecting all relationship between force and displacement, and establish the relationship between force and displacement of cranial cavity

According to the displacement equal principle of the public nodes in all adjacent elements, the relationship between force and displacement of overall cranial cavity collected from the element stiffness matrix:

$$\{F\} = [K]\{\delta\} \quad (2.5)$$

Where: $\{F\}$ - Load array;

[K]- The overall stiffness matrix;

$\{\delta\}$ - The nodal displacement array of the entire cranial cavity.

5) Solve the nodal displacement

After the formula (2.1) ~ (2.5) eliminating the stiffness displacement of geometric boundary conditions, the nodal displacement can be solved from the gathered relationship groups between force and displacement.

6) By classifying the nodal displacement solved from the formula (2.2) and (2.3), the strain

and stress in each element can be calculated.

In this paper, the studied cranial cavity is a hollow three-dimensional sphere, its external radius $R = 100$ mm, the curvature of hollow shell is 0.01 rad/mm, the thickness of shell wall is 6mm, so the element body of hollow spherical can be treated as the regular hexahedron. The following is the stress and strain analyses in the three-dimensional elements in the cranial space. The 8-node hexahedral element (Fig1.3) is used to be the master element. The origin is set up as the local coordinate system (ξ, η, ζ) in the element. Trough the transformation between rectangular coordinates and local coordinates, the space 8-node isoparametric centroid element can be obtained. The relationship of coordinate transformation is:

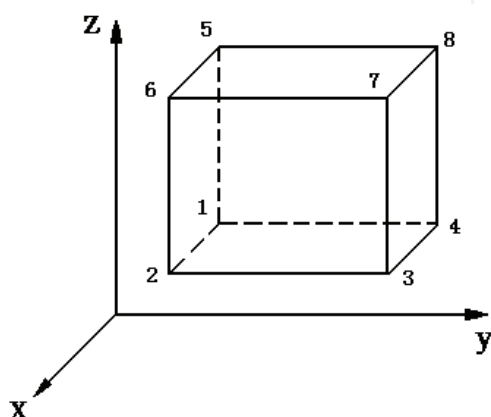


Fig. 2.3 The space 8-node isoparametric centroid element

$$\begin{cases} x = \sum_{i=1}^8 N_i(\xi, \eta, \zeta) x_i \\ y = \sum_{i=1}^8 N_i(\xi, \eta, \zeta) y_i \\ z = \sum_{i=1}^8 N_i(\xi, \eta, \zeta) z_i \end{cases} \quad (2.6)$$

Then the displacement function of element is:

$$\begin{cases} u = \sum_{i=1}^8 N_i(\xi, \eta, \zeta) u_i \\ v = \sum_{i=1}^8 N_i(\xi, \eta, \zeta) v_i \\ w = \sum_{i=1}^8 N_i(\xi, \eta, \zeta) w_i \end{cases} \quad (2.7)$$

Where: x_i 、 y_i 、 z_i and u_i 、 v_i 、 w_i are respectively the coordinate values and actual displacement of nodes.

The element displacement function with matrix is expressed as:

$$\{\delta\} = \begin{Bmatrix} u \\ v \\ w \end{Bmatrix} = \sum_{i=1}^8 \begin{bmatrix} N_i & 0 & 0 \\ 0 & N_i & 0 \\ 0 & 0 & N_i \end{bmatrix} \begin{Bmatrix} u_i \\ v_i \\ w_i \end{Bmatrix} = \sum_{i=1}^8 [N_i] \{\delta_i\} = [N] \{\delta\}^e \quad (2.8)$$

Where: $\{\delta_i\}$ - Nodal displacement array, $\{\delta_i\} = [u_i \ v_i \ w_i]^T$ ($i = 1, 2, \dots, 8$);

$\{\delta\}^e$ - The nodal displacement array of entire element,
 $\{\delta\}^e = [\{\delta_1\} \ \{\delta_2\} \ \dots \ \{\delta_8\}]^T$;

N_i - The uniform shape function of 8 nodes, which can be expressed as:

$$N_i = \frac{1}{8} (1 + \xi_i \xi) (1 + \eta_i \eta) (1 + \zeta_i \zeta) \quad (i = 1, 2, \dots, 8) \quad (2.9)$$

Where: ξ_i , η_i , ζ_i is the coordinates of node i in the local coordinate system (ξ, η, ζ) .

The derivative of composite function to local coordinates is:

$$\begin{cases} \frac{\partial N_i}{\partial \xi} = \frac{1}{8} \xi_i (1 + \eta_i \eta) (1 + \zeta_i \zeta) \\ \frac{\partial N_i}{\partial \eta} = \frac{1}{8} \eta_i (1 + \xi_i \xi) (1 + \zeta_i \zeta) \\ \frac{\partial N_i}{\partial \zeta} = \frac{1}{8} \zeta_i (1 + \xi_i \xi) (1 + \eta_i \eta) \end{cases} \quad (2.10)$$

The strain relationship of space elements is:

$$\{\varepsilon\} = [B] \{\delta\}^e = \sum_{i=1}^8 [B_i] \{\delta_i\} \quad (2.11)$$

The strain matrix $[B]$ of space element:

$$[B_i] = \begin{bmatrix} \frac{\partial N_i}{\partial x} & 0 & 0 \\ 0 & \frac{\partial N_i}{\partial y} & 0 \\ 0 & 0 & \frac{\partial N_i}{\partial z} \\ \frac{\partial N_i}{\partial y} & \frac{\partial N_i}{\partial x} & 0 \\ 0 & \frac{\partial N_i}{\partial z} & \frac{\partial N_i}{\partial y} \\ \frac{\partial N_i}{\partial z} & 0 & \frac{\partial N_i}{\partial x} \end{bmatrix} \quad (2.12)$$

The shape function was derivative to be:

$$\begin{Bmatrix} \frac{\partial N_i}{\partial x} \\ \frac{\partial N_i}{\partial y} \\ \frac{\partial N_i}{\partial z} \end{Bmatrix} = [J]^{-1} \begin{Bmatrix} \frac{\partial N_i}{\partial \xi} \\ \frac{\partial N_i}{\partial \eta} \\ \frac{\partial N_i}{\partial \zeta} \end{Bmatrix} \quad (2.13)$$

The matrix $[J]$ is the three-dimensional Jacobian ratio matrix of coordinate transformation:

$$[J] = \begin{Bmatrix} \frac{\partial x}{\partial \xi} & \frac{\partial y}{\partial \xi} & \frac{\partial z}{\partial \xi} \\ \frac{\partial x}{\partial \eta} & \frac{\partial y}{\partial \eta} & \frac{\partial z}{\partial \eta} \\ \frac{\partial x}{\partial \zeta} & \frac{\partial y}{\partial \zeta} & \frac{\partial z}{\partial \zeta} \end{Bmatrix} = \begin{bmatrix} \sum_{i=1}^8 \frac{\partial N_i}{\partial \xi} x_i & \sum_{i=1}^8 \frac{\partial N_i}{\partial \xi} y_i & \sum_{i=1}^8 \frac{\partial N_i}{\partial \xi} z_i \\ \sum_{i=1}^8 \frac{\partial N_i}{\partial \eta} x_i & \sum_{i=1}^8 \frac{\partial N_i}{\partial \eta} y_i & \sum_{i=1}^8 \frac{\partial N_i}{\partial \eta} z_i \\ \sum_{i=1}^8 \frac{\partial N_i}{\partial \zeta} x_i & \sum_{i=1}^8 \frac{\partial N_i}{\partial \zeta} y_i & \sum_{i=1}^8 \frac{\partial N_i}{\partial \zeta} z_i \end{bmatrix} \quad (2.14)$$

The stress-strain relationship of space elements is:

$$\{\sigma\} = [D]\{\varepsilon\} = [D][B]\{\delta\}^e \quad (2.15)$$

The elasticity matrix $[D]$ is:

$$[D] = \frac{E(1-\mu)}{(1+\mu)(1-2\mu)} \begin{bmatrix} 1 & 0 & 0 & 0 & 0 & 0 \\ \frac{\mu}{1-\mu} & 1 & 0 & 0 & 0 & 0 \\ \frac{\mu}{1-\mu} & \frac{\mu}{1-\mu} & 1 & 0 & 0 & 0 \\ 0 & 0 & 0 & \frac{1-2\mu}{2(1-\mu)} & \frac{\mu}{1-\mu} & \frac{\mu}{1-\mu} \\ 0 & 0 & 0 & 0 & \frac{1-2\mu}{2(1-\mu)} & \frac{\mu}{1-\mu} \\ 0 & 0 & 0 & 0 & 0 & \frac{1-2\mu}{2(1-\mu)} \end{bmatrix} \quad (2.16)$$

The element stiffness matrix from the principle of virtual work is:

$$[k]^e = \iiint_V [B]^T [D][B] dx dy dz = \begin{bmatrix} k_{11} & k_{12} & \cdots & k_{18} \\ k_{21} & k_{22} & \cdots & k_{28} \\ \cdots & \cdots & \cdots & \cdots \\ k_{81} & k_{82} & \cdots & k_{88} \end{bmatrix} \quad (2.17)$$

Where:

$$[k_{ij}] = \iiint_V [B]^T [D][B] dx dy dz = \int_{-1}^1 \int_{-1}^1 \int_{-1}^1 [B]^T [D][B] J d\xi d\eta d\zeta \quad (2.18)$$

The equivalent nodal forces acting on the space element nodes are:

$$\{F\}^e = [k]^e \{\delta\}^e \quad (2.19)$$

Because the internal pressure in the cranial cavity is surface force, the equivalent load for the pressure acting on the element nodes is:

$$\{F_S\}^e = \iint_S [N]^T \{P_S\} dS \quad (2.20)$$

The relationship between force and displacement in the entire cranial cavity is:

$$\{F\} = [K]\{\delta\} \quad (2.21)$$

Then after obtaining the nodal displacement, the stress and strain in each element can be calculated by combining the formula (2.11) and (2.15).

2.2.2 The stress and strain analysis for complex structure of cranial cavity deformation

Cranial cavity is the hollow sphere formed by the skull and the duramater. From the Fig.1.2, there are obvious interfaces among the various parts of outer compact bone, middle cancellous bone, inner compact bone and duramater, which is consistent with the characteristics of composite materials [13]. Four layered composite structure of cranial cavity is almost lamelleted distribution. Therefore, the lamelleted structure is adopted to establish and analyze the finite-element model of cranial cavity, and the laminated shell element is used to describe the thin cranial cavity made up of skull and duramater. Here the cranial cavity deformation of laminated structure is analyzed as follows:

(1) The stress and strain analysis for the single layer of cranial deformation

Each layers of cranial cavity are all thin flat film. The skulls are transversely isotropic material. The thickness of Tabula externa, diploe, Tabula interna, duramater is all very small. So compared with the components in the surface, the stress components are very small along the normal direction, and can be neglected. So the deformation analysis to single-layer cranial cavity can be simplified to be the stress problems of two-dimensional generalized plane.

The stress-strain relationship of each single-layer structure in the cranial cavity:

$$\{\sigma\} = [Q]\{\varepsilon\} \quad (2.22)$$

Namely:

$$\begin{Bmatrix} \sigma_1 \\ \sigma_2 \\ \tau_{12} \end{Bmatrix} = \begin{bmatrix} Q_{11} & Q_{12} & 0 \\ Q_{21} & Q_{22} & 0 \\ 0 & 0 & Q_{66} \end{bmatrix} \begin{Bmatrix} \varepsilon_1 \\ \varepsilon_2 \\ \mu_{12} \end{Bmatrix} \quad (1.23)$$

Where, 1,2 - The main direction of elasticity in the plane;

$[Q]$ - Stiffness matrix, $Q_{11} = mE_1$, $Q_{12} = m\mu_{12}E_2$, $Q_{22} = mE_2$, $Q_{66} = G_{12}$;

$$m = \left(1 - \frac{\mu_{12}^2 E_2}{E_1} \right)^{-1};$$

E_1 、 E_2 - The elastic modulus of four independent surfaces in each layer structure;

G_{12} - Shear modulus;

μ_{12} - Poisson's ratio of transverse strain along the 2 direction that the stress acts on the 1 direction.

(2) The stress and strain analysis for the laminated deformation of cranial cavity

The cranial cavity is as a whole formed by the four-layer structures. So the material, thickness and elastic main direction are all different. The overall performance of cranial cavity is anisotropic, macroscopic non-uniformity along the thickness direction and non-continuity of mechanical properties. Thus, the assumptions need to be made before analyzing the overall deformation of cranial cavity [14]:

1) The same deformation in each layer

Each single layer is strong glued. There are the same deformation, and no relative displacement;

2) No change of direct normal

The straight line vertical to the middle surface in each layer before the deformation remains still the same after the deformation, and the length of this line remains unchanged whether before or after deformation;

3) $\sigma_z = 0$

The positive stress along the direction of thickness is small compared to other stress, and can be ignored;

4) The plane stress state in each single layer

Each single-layer structure is similar to be assumed in plane stress state.

From the four-layer laminated structure composed of Tabula externa, diploe, Tabula interna, duramater, the force of each single-layer structure is indicated in Fig2.4. The middle surface in the laminated structure of cranial cavity is the xy coordinate plane. z axis is perpendicular to the middle surface in the plate. Along the z axis, each layer in turn will be compiled as layer 1, 2, 3, and 4. The corresponding thickness is respectively t_1, t_2, t_3, t_4 . As a overall laminated structure, the thickness of cranial cavity is h , shown in Fig2.5.

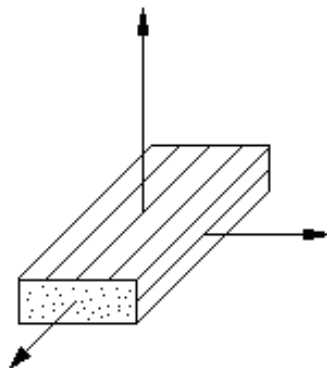


Fig. 2.4 The orientation relationship in each single-layer structure of cranial cavity

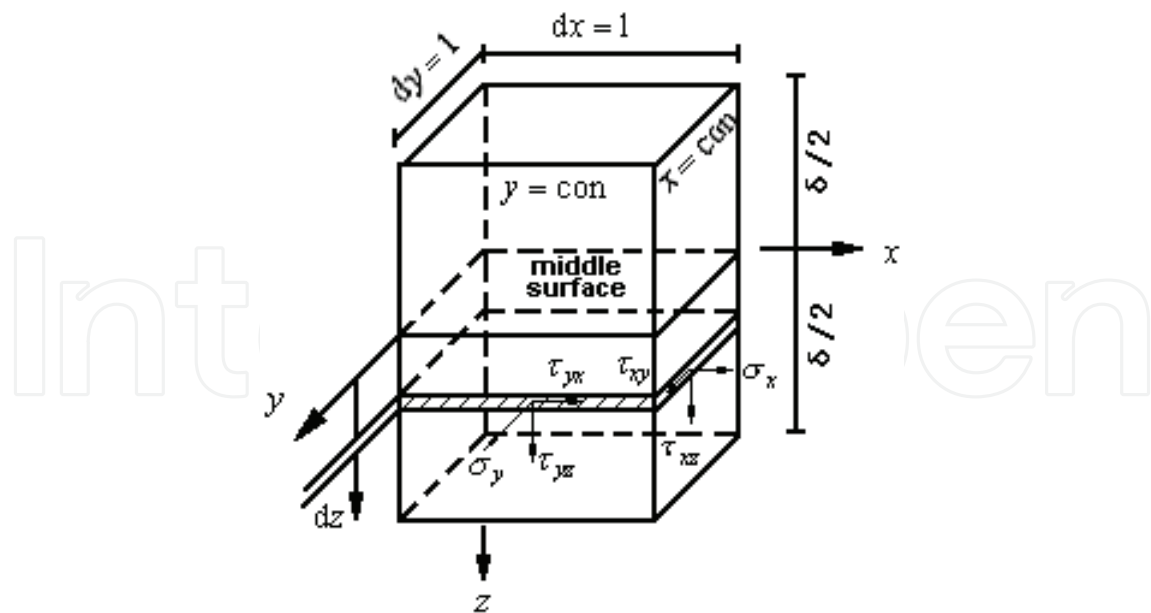


Fig. 2.5 The sketch of four-layered laminated structure of cranial cavity

Then

$$h = \sum_{k=1}^4 t_k \quad (2.24)$$

The z coordinates is respectively z_{k-1} and z_k , then $z_0 = -h/2$ and $z_4 = h/2$.

The displacement components at any point within the laminated structure of cranial cavity:

$$\left. \begin{aligned} u &= u(x, y, z) \\ v &= v(x, y, z) \\ w &= w(x, y, z) \end{aligned} \right\} \quad (2.25)$$

The strain is:

$$\left\{ \begin{aligned} \varepsilon_x &= \frac{\partial u}{\partial x} = \frac{\partial u_0}{\partial x} - z \frac{\partial^2 w}{\partial x^2} \\ \varepsilon_y &= \frac{\partial v}{\partial y} = \frac{\partial v_0}{\partial y} - z \frac{\partial^2 w}{\partial y^2} \\ \gamma_{xy} &= \frac{\partial u}{\partial y} + \frac{\partial v}{\partial x} = \frac{\partial u_0}{\partial y} + \frac{\partial v_0}{\partial x} - 2z \frac{\partial^2 w}{\partial x \partial y} \end{aligned} \right. \quad (2.26)$$

Where: $u = u(x, y, z)$, $v = v(x, y, z)$, $w = w(x, y, z)$ - The displacement components at any point within the cranial cavity;

$u_0(x, y)$, $v_0(x, y)$ - The displacement components in the middle surface;

$w(x, y)$ - Deflection function, the deflection function of each layer is the same.

Fomular (2.26) can be expressed to be in matrix form:

$$\{\varepsilon\} = \{\varepsilon_0\} + z\{k\} \quad (2.27)$$

Where: ε_0 - Strain array in the plane, $\{\varepsilon_0\} = \left[\frac{\partial u_0}{\partial x}, \frac{\partial v_0}{\partial y}, \left(\frac{\partial u_0}{\partial y} + \frac{\partial v_0}{\partial x} \right) \right]^T$;

k - Strain array of bending in the surface, $\{k\} = \left[-\frac{\partial^2 w}{\partial x^2}, -\frac{\partial^2 w}{\partial y^2}, -2\frac{\partial^2 w}{\partial x \partial y} \right]^T$.

The mean internal force and torque acting on the laminated structure of cranial cavity in the unit width is:

$$\begin{cases} N_i = \int_{-h/2}^{h/2} \sigma_i dz \\ M_i = \int_{-h/2}^{h/2} \sigma_i z dz \end{cases} \quad (i = x, y, xy) \quad (2.28)$$

Taking into account the discontinuous stress caused by the discontinuity along the direction of laminated structure in the cranial cavity, the formula (2.28) can be rewritten in matrix form:

$$\begin{cases} \{N\} = \sum_{k=1}^n \int_{z_{k-1}}^{z_k} \{\sigma\} dz \\ \{M\} = \sum_{k=1}^n \int_{z_{k-1}}^{z_k} \{\sigma\} z dz \end{cases} \quad (2.29)$$

After substituting the formula (2.22) and (2.27) into equation (2.29), the average internal force and internal moment of the laminated structure in the cranial cavity is:

$$\begin{Bmatrix} N \\ M \end{Bmatrix} = \begin{bmatrix} \sum \int [Q] dz & \sum \int [Q] z dz \\ \sum \int [Q] z dz & \sum \int [Q] z^2 dz \end{bmatrix} \begin{Bmatrix} \varepsilon_0 \\ k \end{Bmatrix} = \begin{bmatrix} A & B \\ B & D \end{bmatrix} \begin{Bmatrix} \varepsilon_0 \\ k \end{Bmatrix} \quad (2.30)$$

Where: $[A]$ - The stiffness matrix in the plane, $A_{ij} = \sum_{k=1}^n Q_{ij}^{(k)} (z_k - z_{k-1})$;

$[B]$ - Coupling stiffness matrix, $B_{ij} = \frac{1}{2} \sum_{k=1}^n Q_{ij}^{(k)} (z_k^2 - z_{k-1}^2)$;

$[D]$ - Bending stiffness matrix, $D_{ij} = \frac{1}{3} \sum_{k=1}^n Q_{ij}^{(k)} (z_k^3 - z_{k-1}^3)$, $(i, j = 1, 2, 6)$.

Then the flexibility matrix of laminated structure in the cranial cavity is:

$$\begin{bmatrix} a & b \\ c & d \end{bmatrix} = \begin{bmatrix} A & B \\ B & D \end{bmatrix}^{-1} \quad (2.31)$$

Where: $[a] = [A]^{-1} + [A]^{-1}[B]([D] - [B][A]^{-1}[B])^{-1}[B][A]^{-1}$

$[b] = -[A]^{-1}[B]([D] - [B][A]^{-1}[B])^{-1}$

$$[c] = -\left([D] - [B][A]^{-1}[B]\right)^{-1}[B][A]^{-1} = [b]^T$$

$$[d] = \left([D] - [B][A]^{-1}[B]\right)^{-1}$$

Thus, the stress-strain relationship of laminated structure in the cranial cavity is:

$$\begin{Bmatrix} \varepsilon_0 \\ k \end{Bmatrix} = \begin{bmatrix} a & b \\ b^T & d \end{bmatrix} \begin{Bmatrix} N \\ M \end{Bmatrix} \quad (2.32)$$

With the changing ICP, to determine how the viscoelasticity of human skull and duramater influences the strains of human skull respectively by ignoring and considering the viscoelasticity of human skull and duramater, we make the analysis of the actual deformation of cranial cavity by considering the viscoelasticity of human skull-duramater system with the finite-element software MSC_PATRAN/NASTRAN and ANSYS. Considering the complexity to calculate the viscoelasticity of human skull and duramater, we can simplify the calculation while on-line analysis only considering the elasticity but ignoring the viscoelasticity of human skull and duramater after obtaining the regularity how the viscoelasticity influence the deformation of cranial cavity.

2.2.3 The finite-element analysis of strains by ignoring the viscoelasticity of human skull and duramater

The craniospinal cavity may be considered as a balloon. For the purpose of our analysis, we adopted the model of hollow sphere (Fig2.6). We presented the development and validation of a 3D finite-element model intended to better understand the deformation mechanisms of human skull corresponding to the ICP change. The skull is a layered sphere constructed in a specially designed form with a Tabula externa, Tabula interna, and a porous Diploe sandwiched in between. Based on the established knowledge of cranial cavity importantly composed of skull and duramater, a thin-walled structure was simulated by the composite shell elements of the finite-element software [15].

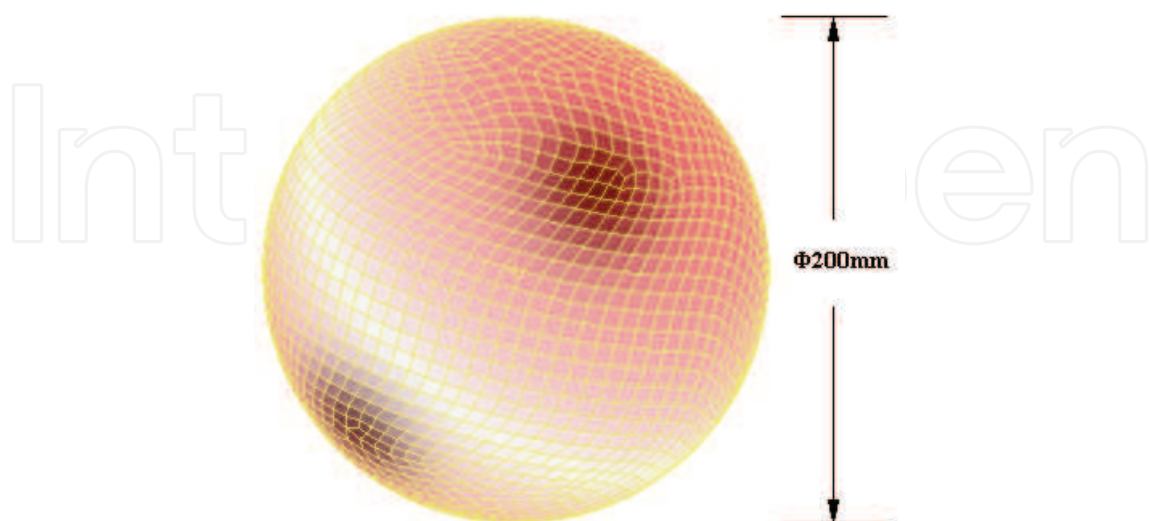


Fig. 6. The sketch of 3D cranial cavity and grid division

Of course, the structure, dimension and characteristic parameter of human skull must be given before the calculation. The thickness of calvaria [16] varies with the position, age, gender and individual, so does dura mater [17]. Tabula externa and interna are all compact bones and the thickness of Tabula externa is more than that of Tabula interna. Diploe is the cancellous bone between Tabula externa and Tabula interna [18]. The parietal bone is the transversely isotropic material, namely it has the mechanical property of rotational symmetry in the axially vertical planes of skull [19]. The important mechanical characteristic of cancellous bone is viscoelasticity, which is generally considered as the semi-closed honeycomb structure composed of bone trabecula reticulation. The main composition of cerebral dura mater, a thick and tough bilayer membrane, is the collagenous fiber which has the characteristic of linear viscoelasticity [20]. And the thickness of dura mater obviously varies with the changing ICP [21]. The mechanical performance of skull is isotropic along the tangential direction on the surface of skull bone [22], in which the performance of compact bone in the Tabula externa is basically the same as that in the Tabula interna [23]. Thus both cancellous bone and dura mater can be regarded as isotropic materials. And the elastic modulus of fresh dura mater varies with the delay time [24].

Next we need determine the fluctuant scope of human ICP. ICP is not a static state, but one that influenced by several factors. It can rise sharply with coughing and sneezing, up to 50 or 60mmHg to settle down to normal values in a short time. It also varies according to the activity the person is involved with. For these reasons single measurement of ICP is not a true representation. ICP needs to be measured over a period. Measured by means of a lumbar puncture, the normal ICP in adults is 8 mmHg to 18 mmHg. But so far there are almost no records of the actual human being's ICP in clinic. The geometry and structure of monkey's skull, mandible and cervical muscle are closer to those of human beings than other animals'. So the ICP of monkeys [25] can be taken as the reference to that of human beings'. The brain appears to be mild injury when ICP variation is about 2.5 kPa, moderate injury when ICP variation is about 3.5 kPa and severe injury when ICP variation is about or more than 5 kPa. Therefore, we carried out the following theoretical analysis with the ICP scope from 1.5 kPa to 5 kPa.

In this paper, the finite-element software MSC_PATRAN/NASTRAN and ANSYS are applied to theoretically analyze the deformation of human skull with the changing ICP. The external diameter of cranial cavity is about 200 mm. The thickness of shell is the mean thickness of calvarias. The average thickness of adult's calvaria is 6.0 mm, that of Tabula externa is 2.0 mm, diploe is 2.8 mm, Tabula interna is 1.2 mm and, dura mater in the parietal position is 0.4 mm.

Considering the characteristic of compact bone, cancellous bone and dura mater, we adopt their elastic modulus and Poisson ratios as 1.5×10^4 MPa, 4.5×10^3 MPa [26], 1.3×10^2 MPa [27] and 0.21, 0.01, 0.23 respectively.

After ignoring the viscoelasticity of human skull and dura mater, the strains of cranial cavity are shown in Table 1 with the finite-element software MSC_PATRAN/NASTRAN as ICP changing from 1.5 kPa to 5.0 kPa (Fig2.7). There is the measurable correspondence between skull strains and ICP variation. The strains of human skull can reflect the ICP change. When ICP variation is raised up to 2.5 kPa, the stress and strain graphs of skull bone are shown in Fig2.8~Fig2.13.

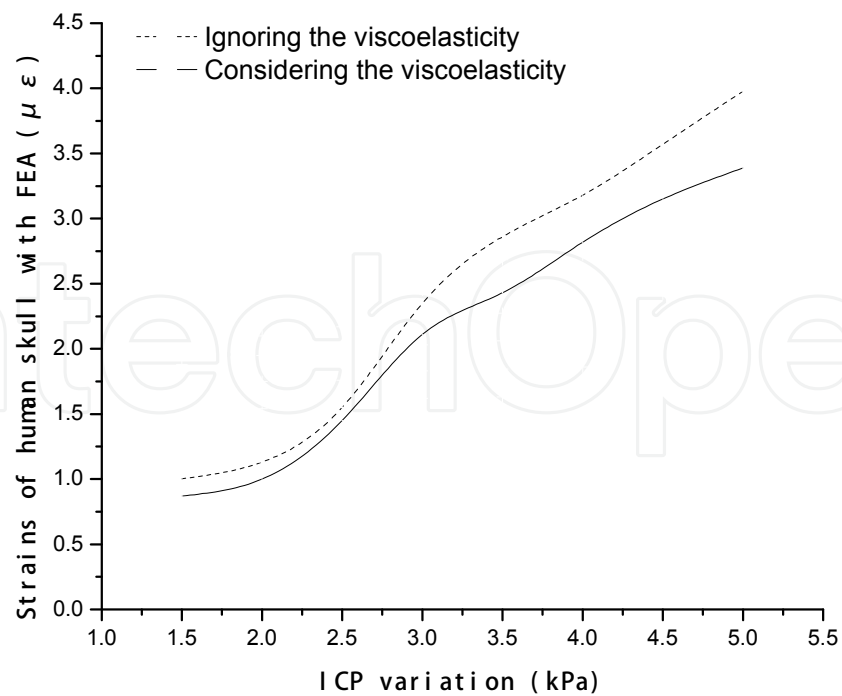


Fig. 2.7 The strain curves of finite-element simulation under the conditions of ignoring and considering the viscoelasticity of human skull and duramater with the changing ICP from 1.5kPa to 5kPa

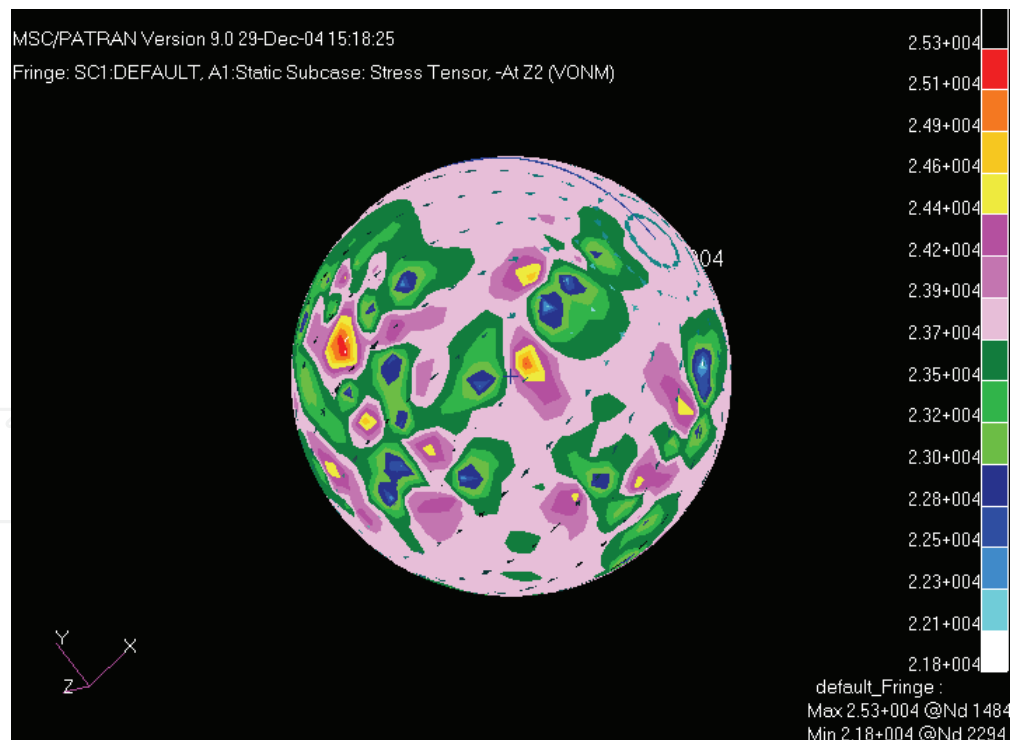


Fig. 2.8 Stress distribution

The scope of stress change on the outside surface is from 22.1 kPa to 25.3 kPa when ICP variation is raised up to 2.5 kPa by ignoring the viscoelasticity of human skull and duramater.

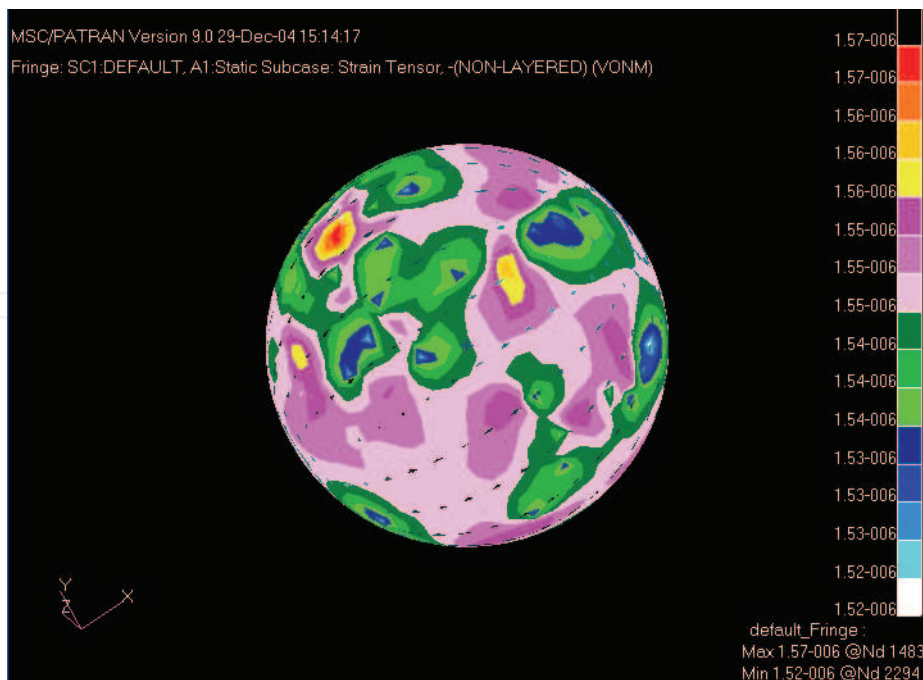


Fig. 2.9 Strain distribution

The scope of strain change on the outside surface is from $1.52\mu\epsilon$ to $1.57\mu\epsilon$ when ICP variation is raised up to 2.5 kPa by ignoring the viscoelasticity of human skull and dura mater.

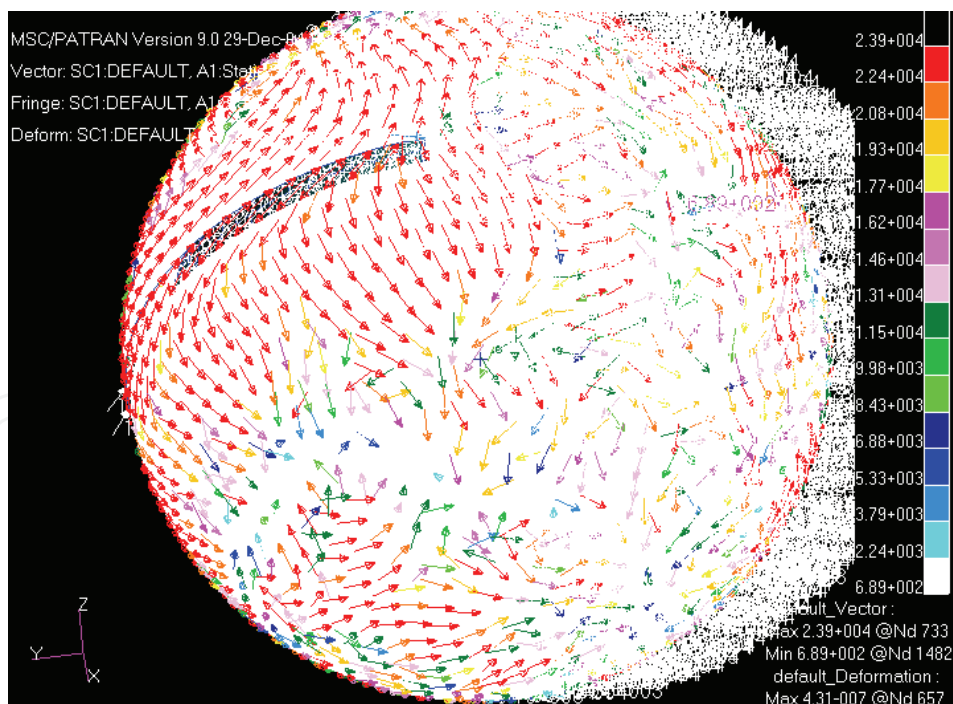


Fig. 2.10 The maximal stress vector distribution

The maximal main stress is about 22.4kPa when ICP variation is raised up to 2.5 kPa by ignoring the viscoelasticity of human skull and dura mater.

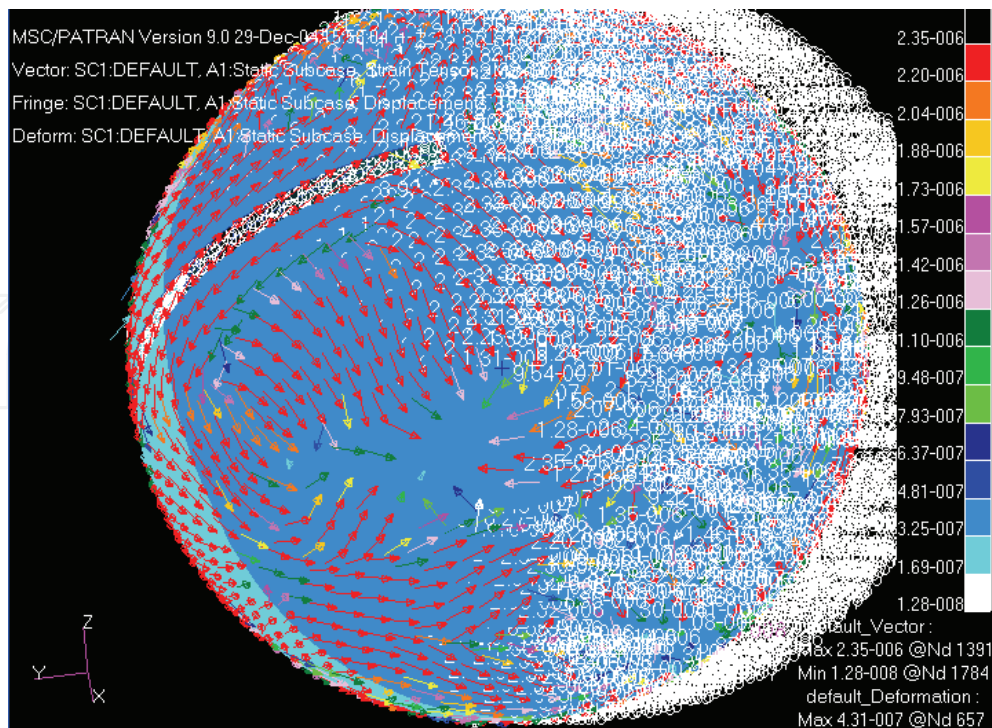


Fig. 2.11 The maximal strain vector distribution

The maximal main strain is about $2.2\mu\epsilon$ when ICP variation is raised up to 2.5 kPa by ignoring the viscoelasticity of human skull and dura mater.

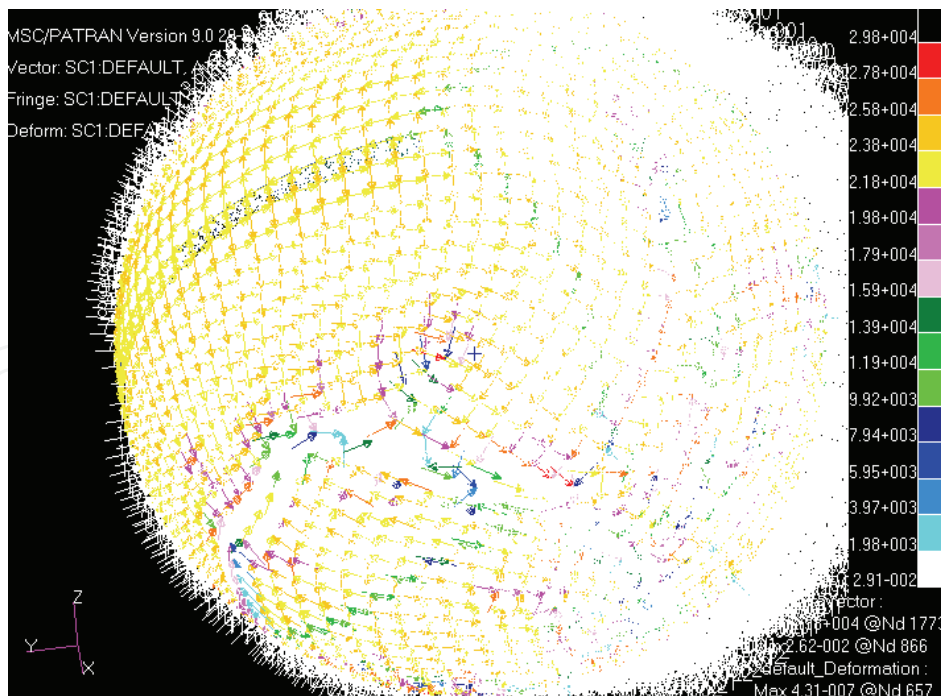


Fig. 2.12 Stress vector distribution

The main stress vector is about 21.8kPa when ICP variation is raised up to 2.5 kPa by ignoring the viscoelasticity of human skull and dura mater.

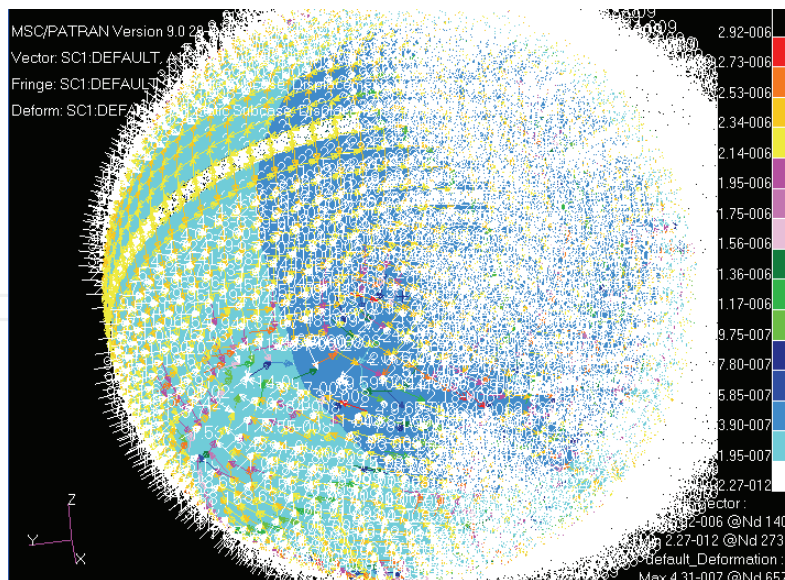


Fig. 2.13 Strain vector distribution

The main strain vector is about $2.14 \mu\epsilon$ when ICP variation is raised up to 2.5 kPa by ignoring the viscoelasticity of human skull and dura mater.

2.2.4 The finite-element analysis of strains by considering the viscoelasticity of human skull and dura mater

Human skull has the viscoelastic material [28]. Considering the viscoelasticity of human skull and dura mater, we use the viscoelastic option of the ANSYS finite-element program to analysis the strains on the exterior surface of human skull as ICP changing. According to the symmetry of 3D model of human skull, the preprocessor of the ANSYS finite-element program is used to construct a 1/8 finite-element model of human skull and dura mater consisting of 25224 nodes and 24150 three-dimensional 8-node isoparametric solid elements, shown in Fig2.10.

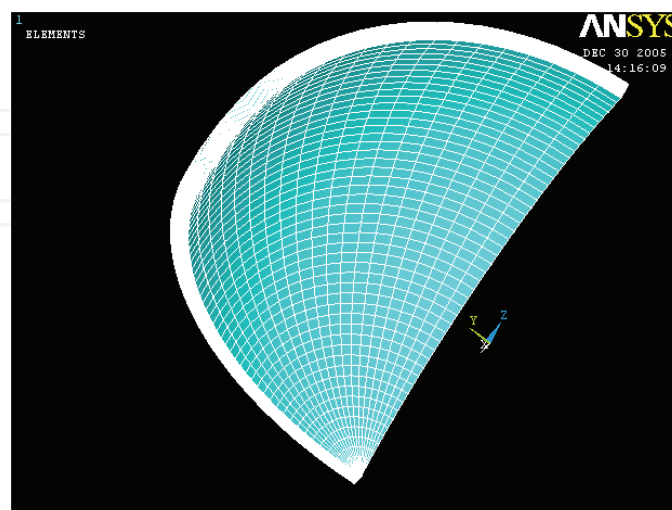


Fig. 2.14 Finite element model of 1/8 cranial cavity shell

The three-dimensional stress-strain relationships for a linear isotropic viscoelastic material are given by:

$$\sigma_{ij} = \int_0^t \left[2G(t-\tau) \frac{\partial e_{ij}(\tau)}{\partial \tau} + \delta_{ij} K(t-\tau) \frac{\partial \theta(\tau)}{\partial \tau} \right] d\tau; \quad (i, j = 1, 2, 3) \quad (2.33)$$

Here, σ_{ij} – – the Cauchy stress tensor;

e_{ij} – – the deviatoric strain tensor;

δ_{ij} – – the Kronecker delta;

$G(t)$ – – the shear relaxation function;

$K(t)$ – – the bulk relaxation function;

$\theta(t)$ – – the volumetric strain;

t – – the present time;

τ – – the past time.

Before the theoretical analysis of the minitraumatic strain-electrometric method, we need to set up the viscoelastic models to describe the relevant mechanical properties of human skull and dura mater.

(1) Viscoelastic model of human skull

Under the constant action of stress, the strain of ideal elastic solid is invariable and that of ideal viscous fluid keeps on growing at the equal ratio with time. However, the strain of actual material increases with time, namely so-called creep. Generally, Maxwell and Kelvin models are the basic models to describe the performance of viscoelastic materials. Maxwell model represents in essence the liquid. Despite the representative of solid, Kelvin model can't describe stress relaxation but only stress creep (Fig2.11). So the combined models made up of the primary elements are usually adopted to describe the viscoelastic performance of actual materials. The creep of linear viscoelastic solid can be simulated by the Kelvin model of three parameters or the generalized Kelvin model.

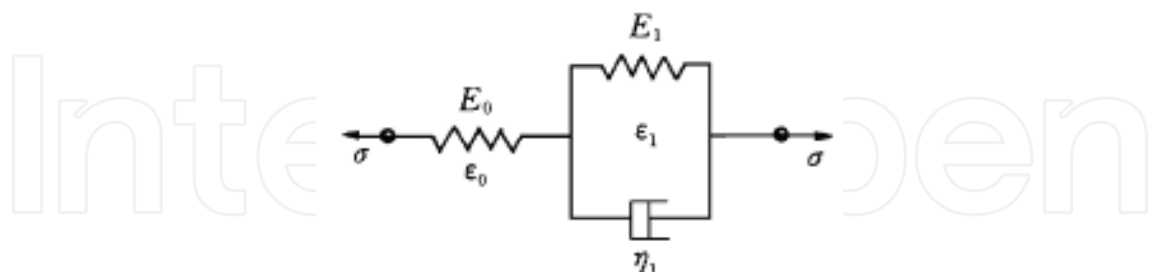


Fig. 2.15 Three parameters Kelvin model of human skull.

Kelvin model of three parameters is shown in Fig2.12 (a). Fig2.12 (b) is the relaxation curves of human skull and Kelvin model of three parameters in the compressive experiment. Fig2.10 (c) is the creep curves of human skull and Kelvin model of three parameters. It shows that the theoretical Kelvin model of three parameters can well simulate the mechanical properties of human skull in the tensile experiments. Thus the Kelvin model of three parameters is adopted to describe the viscoelasticity of human skull in this paper.

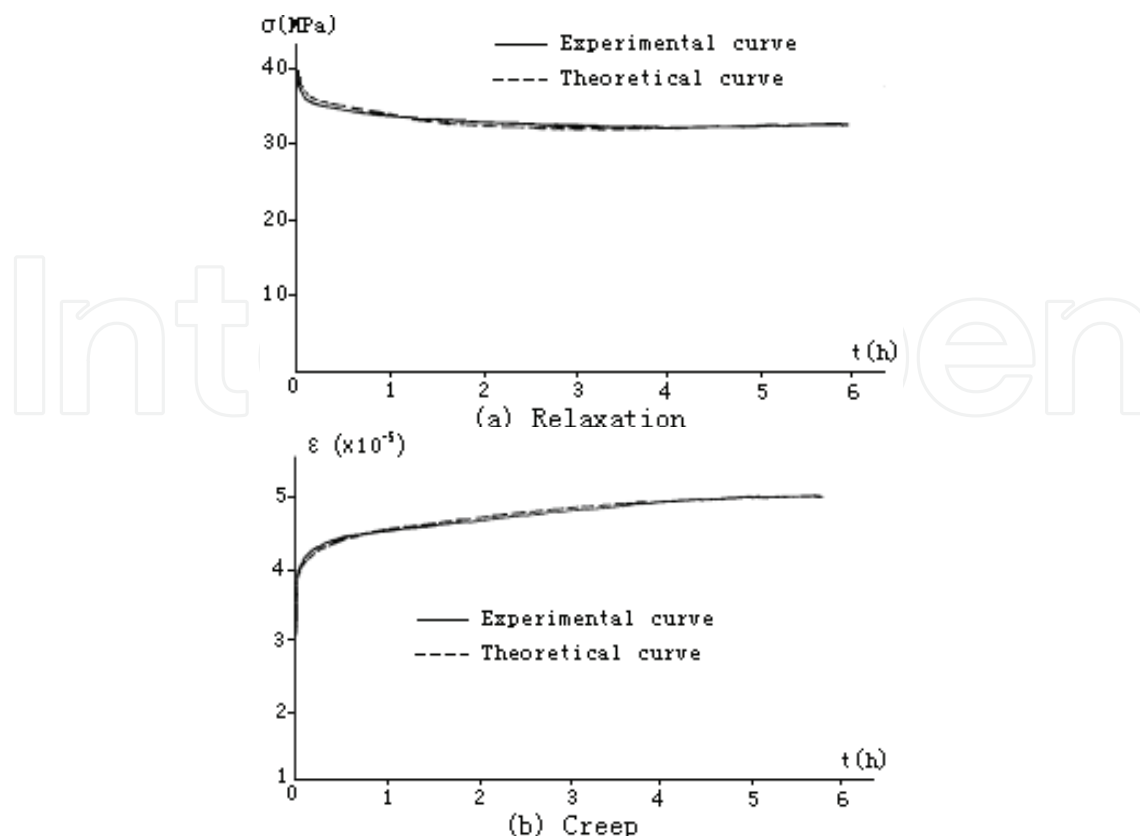


Fig. 2.16 The relaxation and creep train-time curves between experiment and three parameters Kelvin theoretical model of human skull.

For the Kelvin model of three parameters, the stress and strain of human skull are shown in equation (2.34),

$$\begin{cases} \varepsilon = \varepsilon_0 + \varepsilon_1 \\ \sigma = E_1 \varepsilon_1 + \eta \dot{\varepsilon}_1 \\ \sigma = E_0 \varepsilon_0 \end{cases} \quad (2.34)$$

After the calculation based on the equation (1), the elastic modulus of human skull is equation (2.35),

$$E = \left(\frac{E_0 E_1}{E_0 + E_1} \right) + \left(\frac{E_0^2}{E_0 + E_1} \right) e^{\frac{t}{P_1}} \quad (2.35)$$

Here, σ — Direct stress acted on elastic spring or impact stress acted on viscopot;

ε — Direct strain of elastic spring;

E — Elastic modulus of tensile compression;

η — Viscosity coefficient of viscopot;

$\dot{\varepsilon}$ — strain ratio;

$$P_1 = \frac{\eta}{E_0 + E_1}$$

(2) Viscoelastic model of human duramater

The generalized Kelvin model is shown in Fig.2.13 (c). Fig.2.13 (a) is the creep experimental curves of human duramater. Fig.2.13 (b) is the curves of creep compliance for the generalized Kelvin model. It shows that the tendency of creep curve in the experiment is coincident with that of creep compliance for the generalized Kelvin model. Creep is the change law of material deformation with time under the invariable stress, so here σ is constant. For the generalized Kelvin model, the stress-strain relationship is $\varepsilon(t) = J(t)\sigma$. Thus the tendency of theoretical creep curve is totally the same as that of experimental one for human duramater. So in this paper, the generalized Kelvin model composed of three Kelvin-unit chains and a spring is adopted to simulate the viscoelasticity of human dura mater in this paper.

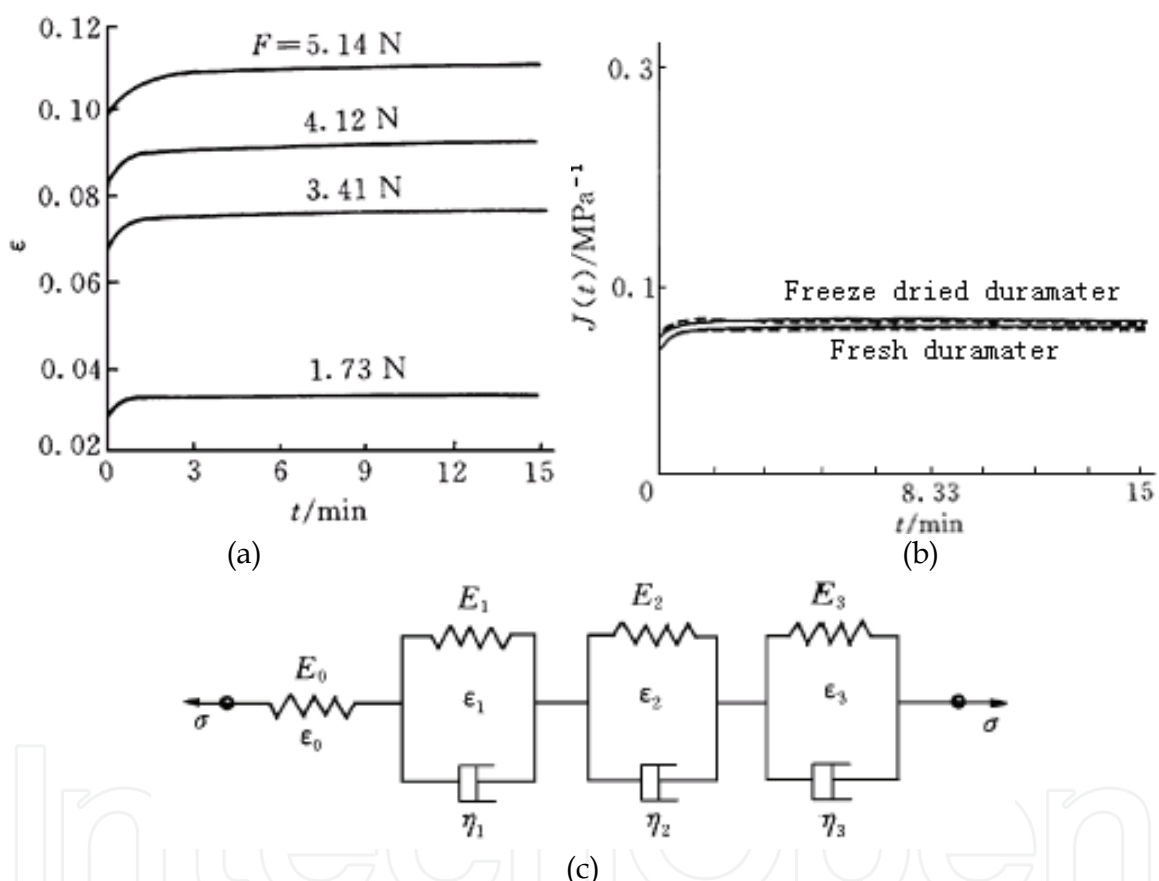


Fig. 2.17 Creep train-time curves under different loads for fresh human duramater ($L_0=23\text{mm}$, $\theta=37^\circ\text{C}$). Creep compliance curves of human duramater Kelvin model. And the Kelvin model of the duramater.

For the viscoelastic model of human dura mater composed of the three Kelvin-unit chains and a spring, the stress and strain of human dura mater are shown in equation (2.36),

$$\begin{cases} \varepsilon = \varepsilon_0 + \varepsilon_1 + \varepsilon_2 + \varepsilon_3 \\ \varepsilon_0 = \frac{\sigma}{E_0} \\ \sigma = E_1\varepsilon_1 + \eta_1\dot{\varepsilon}_1 = E_2\varepsilon_2 + \eta_2\dot{\varepsilon}_2 = E_3\varepsilon_3 + \eta_3\dot{\varepsilon}_3 \end{cases} \quad (2.36)$$

After the calculation based on the equation (2.36), the creep compliance of human dura mater is equation (2.37),

$$J(t) = E_0^{-1} + E(1 - e^{-t/\tau_1}) + E_2^{-1}(1 - e^{-t/\tau_2}) + E_3^{-1}(1 - e^{-t/\tau_3}) \quad (2.37)$$

Then the elastic modulus of human dura mater is equation (5),

$$E = \left[E_0^{-1} + E_1^{-1}(1 - e^{-t/\tau_1}) + E_2^{-1}(1 - e^{-t/\tau_2}) + E_3^{-1}(1 - e^{-t/\tau_3}) \right]^{-1} \quad (2.38)$$

Here, σ , ε , E , η , $\dot{\varepsilon}$ — Ditto mark;

τ_1 , τ_2 , τ_3 — Lag time, that is $\tau_1 = \eta_1 / E_1$, $\tau_2 = \eta_2 / E_2$, $\tau_3 = \eta_3 / E_3$.

In the finite-element software ANSYS, there are three kinds of models to describe the viscoelasticity of actual materials, in which the Maxwell model is the general designation for the combined Kelvin and Maxwell models. Considering the mechanical properties of human skull and dura mater, we adopt the finite-element Maxwell model to simulate the viscoelasticity of human skull-dura mater system. The viscoelastic parameters of human skull and dura mater are respectively listed in Table 2.1 and Table 2.2.

	Elastic Modulus (GPa)		Viscosity (GPa/s)	Delay time τ (s)	
	E0	E1	η	τ_r^*	τ_d^*
Compression	5.69±0.26	42.24±2.09	26.9±1.5	2022±198	2292±246
Tension	13.64±0.59	51.45±2.54	57.25±4.27	3180±300	4026±372

$$* \tau_r = \eta / (E_1 + E_2), \quad \tau_d = \eta / E_2$$

Table 1. Coefficients for the viscoelastic properties for human skull

	Elastic modulus (MPa)				Delay time τ (s)		
	E0	E1	E2	E3	τ_1	τ_2	τ_3
Duramater	16.67	125.0	150.0	93.75	40	10 ⁴	10 ⁶

Table 2. Creep coefficients for the viscoelastic properties for fresh human duramater

(3) The stress and strain distribution by the finite-element analysis

Fig2.14 (a) ~ (e) are the analytic graphs of stress and strain with finite-element software ANASYS when ICP variation is raised up to 2.5kPa. After considering the viscoelasticity of human skull and duramater, the stresses and strains of cranial cavity are shown in Fig2.15 as the ICP changing from 1.5kPa to 5kPa with the finite-element software ANSYS. It shows that the stress and strain distributions on the exterior surface of human skull are well-proportioned and that the stress and strain variation on the exterior surface of cranial cavity is relatively small corresponding to the ICP change. The strains of cranial cavity are

coincident with ICP variation. The deformation scope of human skull is theoretically from $0.9 \mu\epsilon$ to $3.4 \mu\epsilon$ as the ICP changing from 1.5kPa to 5.0kPa. Corresponding to ICP of 2.5kPa, 3.5kPa and 5.0kPa, the strain of skull deformation separately for mild, moderate and severe head injury is $1.5 \mu\epsilon$, $2.4 \mu\epsilon$, and $3.4 \mu\epsilon$ or so.

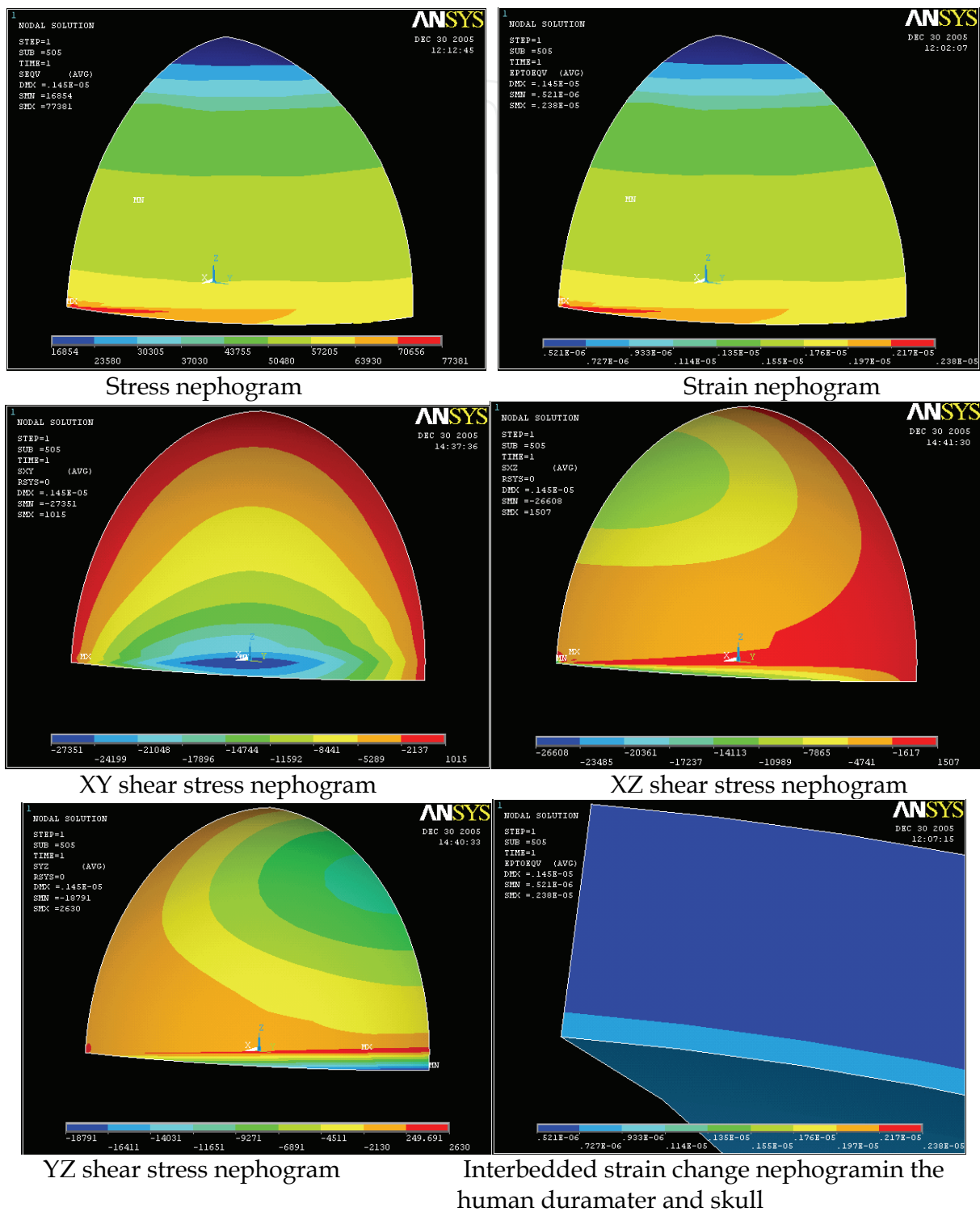


Fig. 2.18 The stress and strain distribution considering viscoelasticity of human skull and duramater

From the relationships about total, elastic and viscous strains of human skull and dura mater in Fig.4 (g), the viscous strains account for about 40% and the elastic strains are about 60% of total strains with the increasing ICP.

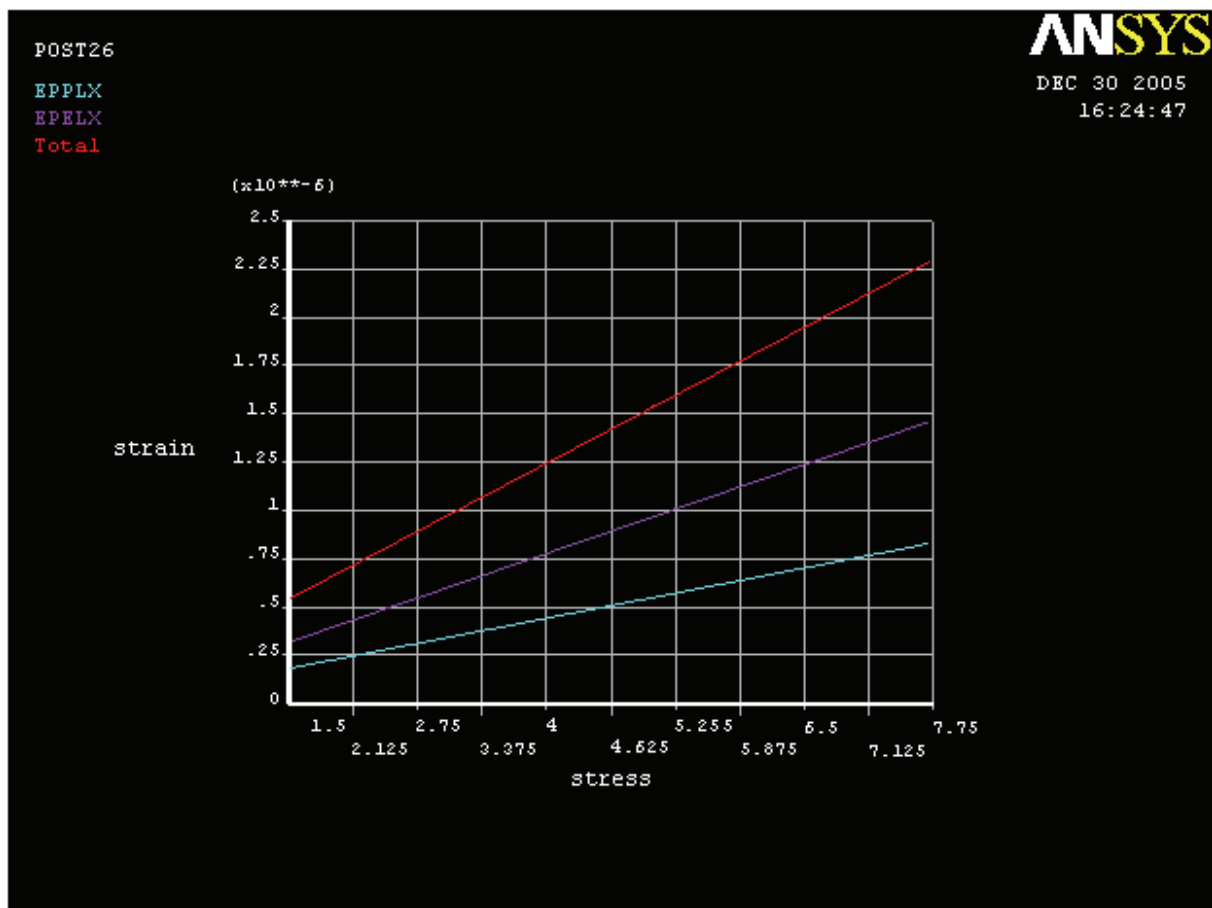


Fig. 2.19 Curves among total, elastic and viscous strain when the ICP increment is 2.5kPa. Here EPPLX is elastic strain curve, EPPLX is viscous strain curve. The viscous strain is about 40% of total strain.

3. Potential Therapeutic Actions of Hypothermia

Intracranial pressure (ICP) is a main index and extremely important to the diagnoses and treatment of many diseases in neurosurgery. Acute cerebral diseases frequently lead to elevated ICP that is the early signal of illness complication in the skull and the common reason of death in the advanced stage, and intracranial pressure has been higher than 2.0kPa (15mmHg) [29]. An increase in ICP is a severe medical problem. The diseases of central nervous system, such as severe head injury, cerebrovascular accident, brain tumor, etc, can cause various central high fevers, often up to 39°C or above [30], which have serious adverse effects on the disease prognosis. Because the increased ICP affects the thermoregulation center of hypothalamus, a sustained high fever will be appeared in clinic, often up to 39°C or above [31]. Mild hypothermia therapy can significantly improve the recovery of the central nervous system, has a positive effect on the treatment of severe head

injury, can reduce intracranial hypertension and mortality, and improve the prognosis [32]. Thus, the mild hypothermia is the main temperature environment for the treatment of brain injury, intracranial hypertension, and so on. Mild hypothermia treatment of severe traumatic brain injury in recent years is another important means [33].

Yue et al [34,35] proved the human skull and duramater could be deformed with the changing ICP, and the deformation scope of human skull is from $1.30\ \mu\epsilon$ to $4.80\ \mu\epsilon$ as the ICP changing from 1.5 kPa to 5.0 kPa. The deformation tendency in this paper needs to be studied with the increasing ICP under the mild hypothermia environment.

The finite-element method extensively solves the biomechanical problem in the medical fields. Compared to other bio-mechanical modelling, the finite-element method can more accurately express the human body geometry and architecture. Therefore, the ANSYS finite-element software is in this paper used to reconstruct the three-dimensional cranial cavity of human being with the mild hypothermia treatment.

3.1 Methods

3.1.1 The geometric model

Reconstruction of the finite-element model of cranial cavity are mostly through the multi-CT scanning technology at home and abroad [36, 37], which is simple and high precision. However, the object being scanned is only a single individual. It is difficult to scan multiple images of individual unity for the universal data. Based on the average measured data of human skull of 104 Chinese people from 18 to 76 years of age, including 67 male and 37 female [38], the three-dimensional model of cranial cavity are directly drawn in the ANSYS program.

This paper studied importantly the deformation of cranial cavity, including brain tissue, cerebrospinal fluid and brain blood flow with the ICP changes. So the model of cranial cavity was properly simplified: only the cavity in which the brain lies, that is, a closed cavity is made up of the parietal bone, occipital, frontal and temporal bone, and a layer of duramater. For the approximate symmetry of person's head, the 1/2 cranial cavity model is built in this paper (Fig3.1).

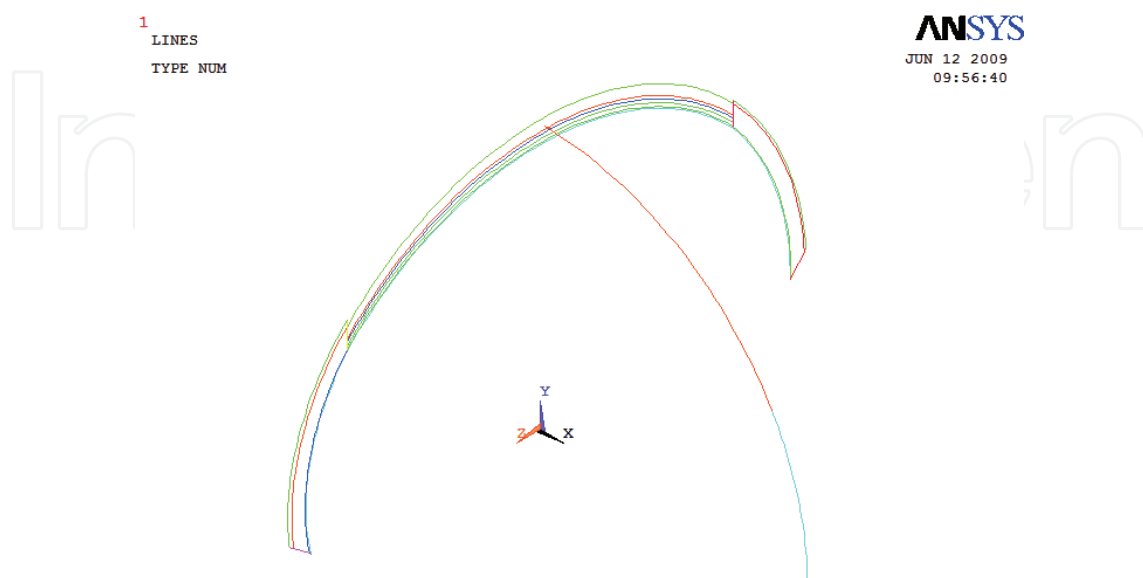


Fig. 3.1 Skeleton of the cranial cavity trendline

In Fig3.1, the thickness of parietal, frontal, occipital, temporal bone, as well as duramater are respectively 5.3560mm, 6.5558mm, 7.5286mm, 2mm and 0.4mm [39, 40]. From outside to inside each layer in turn, the thickness of external compact bone, diploe and internal compact bone are about 3mm, 1.8mm, 1mm. Due to the smoothness, the parietal bone is regarded as the main measured position. By the Extrude command, the Fig.1 can be formed the volume. After bonding the border among the frontal, parietal, occipital and temporal bone and the duramater with the glue command, the model of cranial cavity is shown in Fig3.2.

3.1.2 The meshing and load

Although the thickness is only 0.4mm [41], the viscoelasticity of duramater is strong [42], so the effect is great on the cranial deformation. The three-dimensional finite element model of cranial cavity is dealt with a composite structure made up of the skull and duramater. The elastic modulus and Poisson's ratio of parietal bone, frontal bone and other parts is shown in Table 3.1. The hexahedral grid was adopted to mesh the entire cranial cavity. The adjacent parts were dealt with the Glue command, and the grid refinement with the Meshing-Modify Mesh command were used as the irregular mesh to the edge, sharp or irregular position. Thus the 1/2 finite-element model of the cranial cavity, including the parietal, pre-frontal, occipital, temporal bone and duramater, and the cell type is block unit. The Fig3.3 is the meshing diagram of 1/2 cranial cavity, in which there are 9,700 hexahedral element and 27,256 nodes.

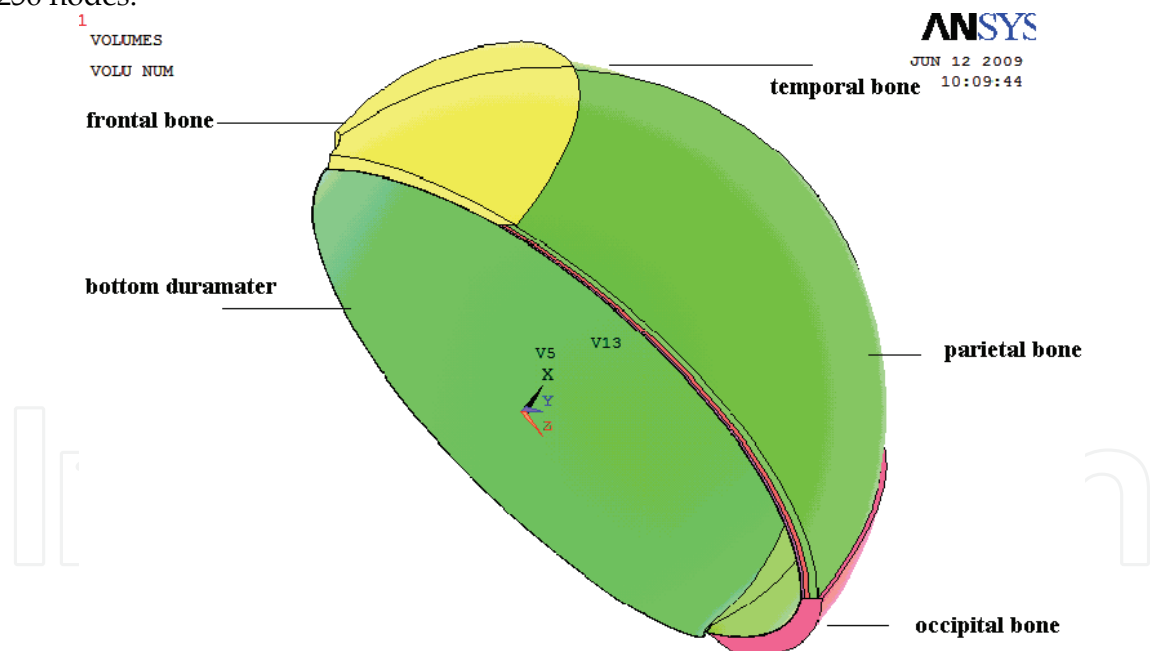


Fig. 3.2 3D model of 1/2 cranial cavity

	Elastic modulus	Poisson's ratio
Parietal bone		
Compact bone	$1.5 \times 10^{10} \text{Pa}$	0.21
Cancellous bone	$4.5 \times 10^9 \text{Pa}$	0.01
Duramater	$1.3 \times 10^8 \text{Pa}$	0.23

Table 3. [43, 44] The material characteristics of human skull and duramater

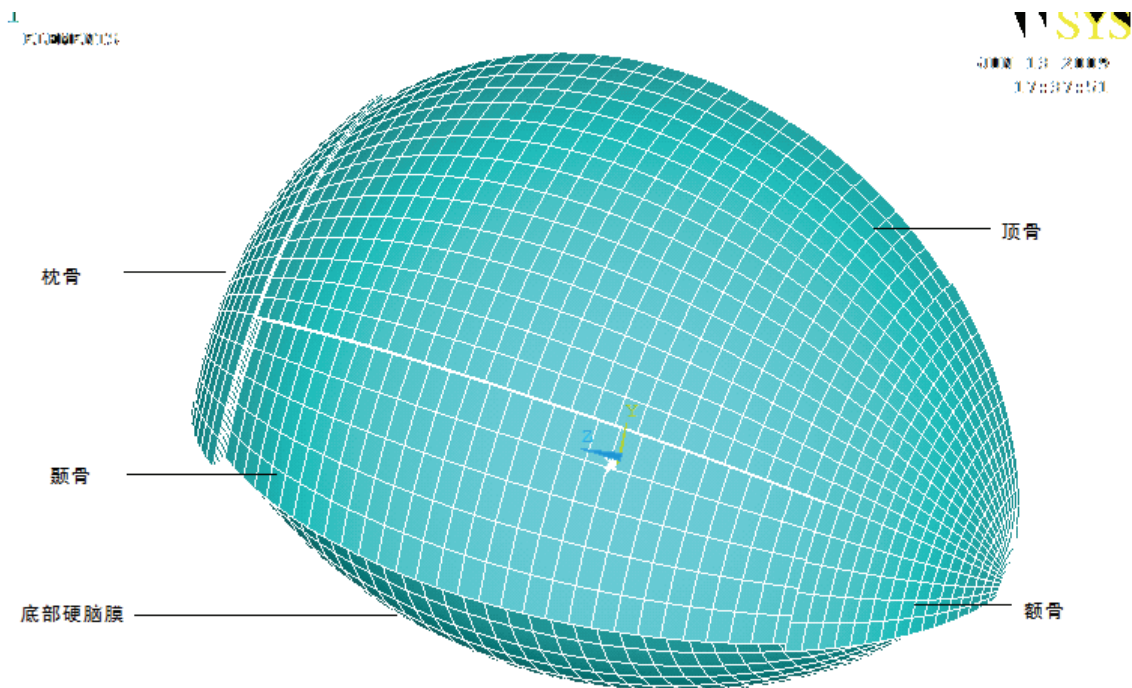


Fig. 3.3 Finite-element meshes of 1/2 cranial cavity

According to the literature [45], the scope of increased intracranial pressure is refined from 2.0kPa to 6.0kPa. Namely, the outward loads among 2.0kPa ~ 6.0kPa are imposed on the inside surfaces of the cranial cavity model to simulate the ICP changes. The temperature of high fever caused by the Intracranial hypertension is 39.5°C [30], which is the initial temperature inside the cranial cavity. The medical definition range of mild hypothermia is from 28°C to 35°C [46]. The over-temperature protection will make the protective effect isn't obvious. If the treatment temperature is too low, the serious complications will come into being. So the optimal temperature of treatment are consistent with the scope among 32°C ~ 35°C at home and abroad [47]. The average 33.5°C is the set point in this paper. In Clinic, the ice bag or blanket wrapped around the patients' body is used to cool the temperature during the mild hypothermia therapy [49]. Thus the temperature load of 33.5°C is exerted to the outer surface of human skull to simulate the mild hypothermia therapy.

3.2 Results

While patients have high fever or are in the mild hypothermia treatment, Fig3.4 - Fig3.7 are separately the strain graphs corresponding to ICP of 2.5kPa and 5.0kPa. And the Table 3.2 is the relevant data of finite-element simulation. Based on the above graphs and charts, it shows that the strains of human skull are in agreement with ICP variation whether under the high fever or mild hypothermia environments. But the former is slightly lower than the latter. At the same time, the strains of junction between the occipital and frontal parietal bone is the maximum, the connecting with the temporal bone is smaller, and the strains lie in the middle level at the central part of parietal bone.

Fig3.4 and Fig3.5 are the respectively strain diagrams of cranial cavity under the mild hypothermia environment and normal temperature conditions while the ICP is 3.0kPa. It

shows that the strains decreased about $0.001\mu\epsilon$ under the mild hypothermia environment than those under the normal temperature conditions during the same circumstance of ICP changes.

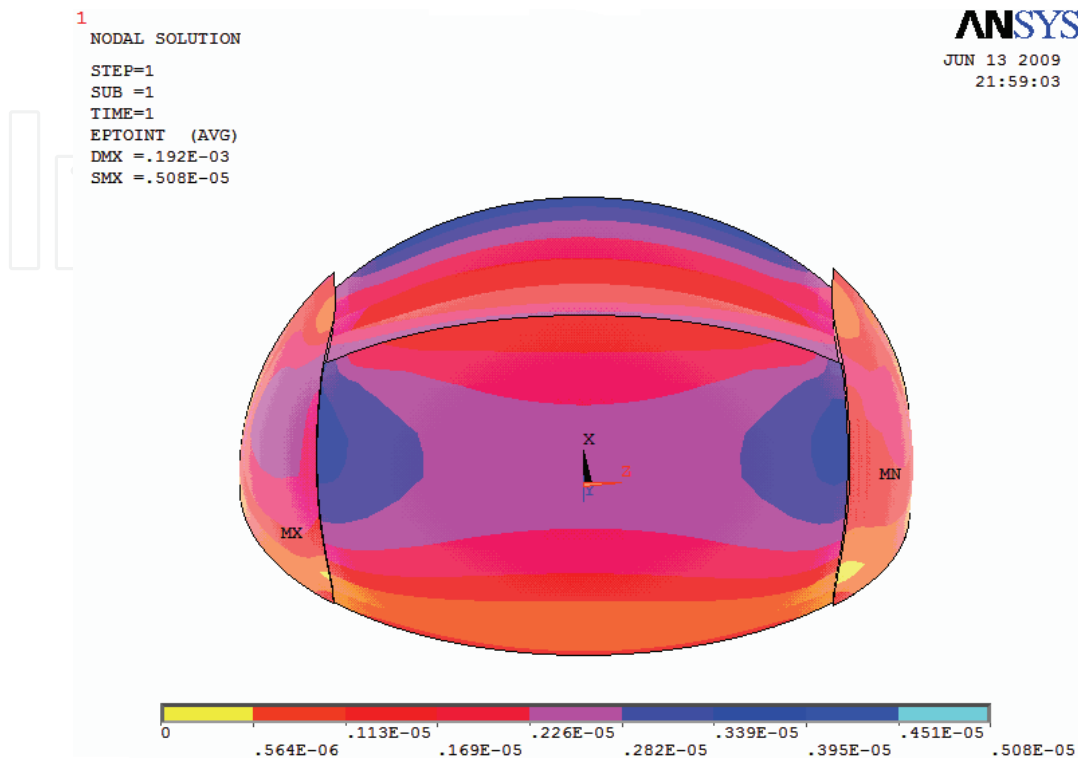


Fig. 3.4 Strain graph without hypothermia treatment when the ICP is 3.0kPa

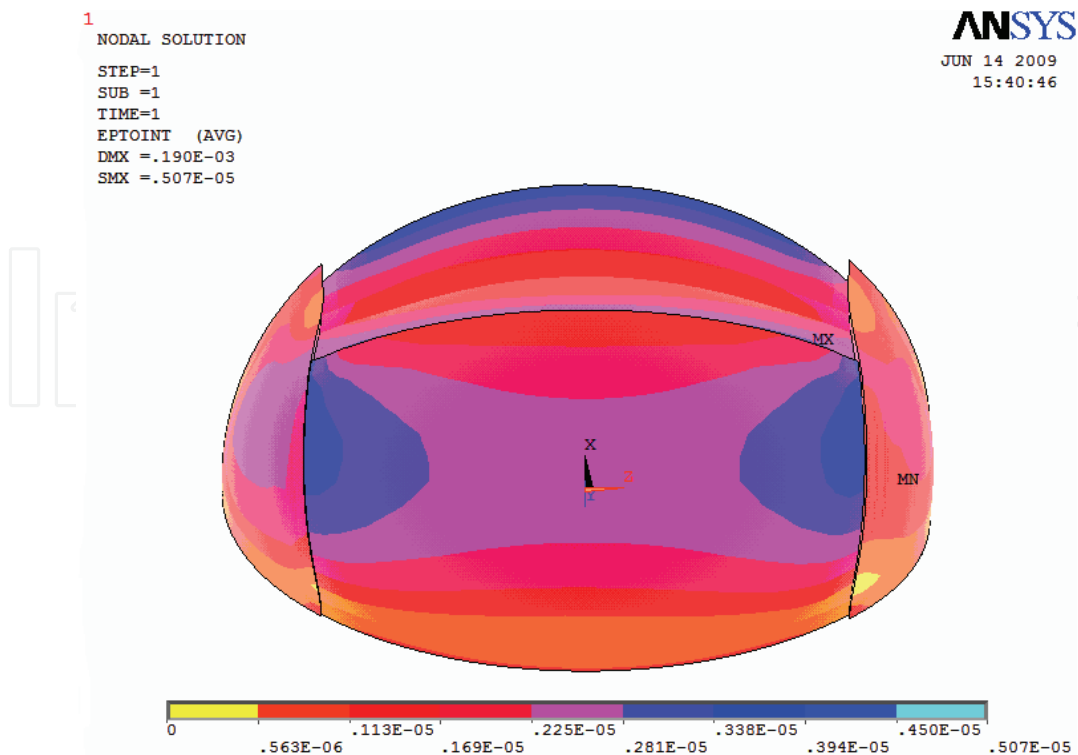


Fig. 3.5 Strain graph with hypothermia treatment when the ICP is 3.0kPa

Fig3.6 and Fig3.7 are the respectively strain diagrams of cranial cavity under the mild hypothermia environment and normal temperature conditions while the ICP is 5.0kPa. It shows that the deformation strains of cranial cavity were significantly increased with the rising ICP. The strains increased while ICP is 3.0kPa about 39.9% than those while ICP is 5.0kPa under the normal temperature conditions. Moreover, the strains decrease more obviously under the mild hypothermia environment, and the maximum is $0.03\mu\epsilon$ appeared in the junction among the parietal, frontal and occipital bone.

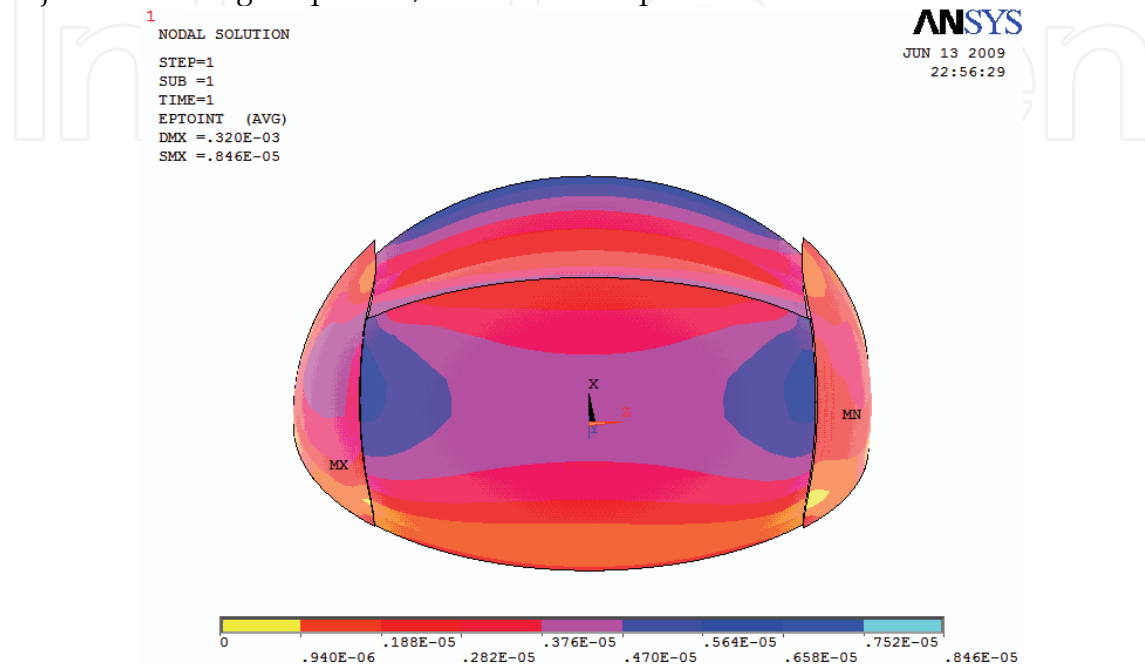


Fig. 3.6 Strain graph without hypothermia treatment when the ICP is 5.0kPa

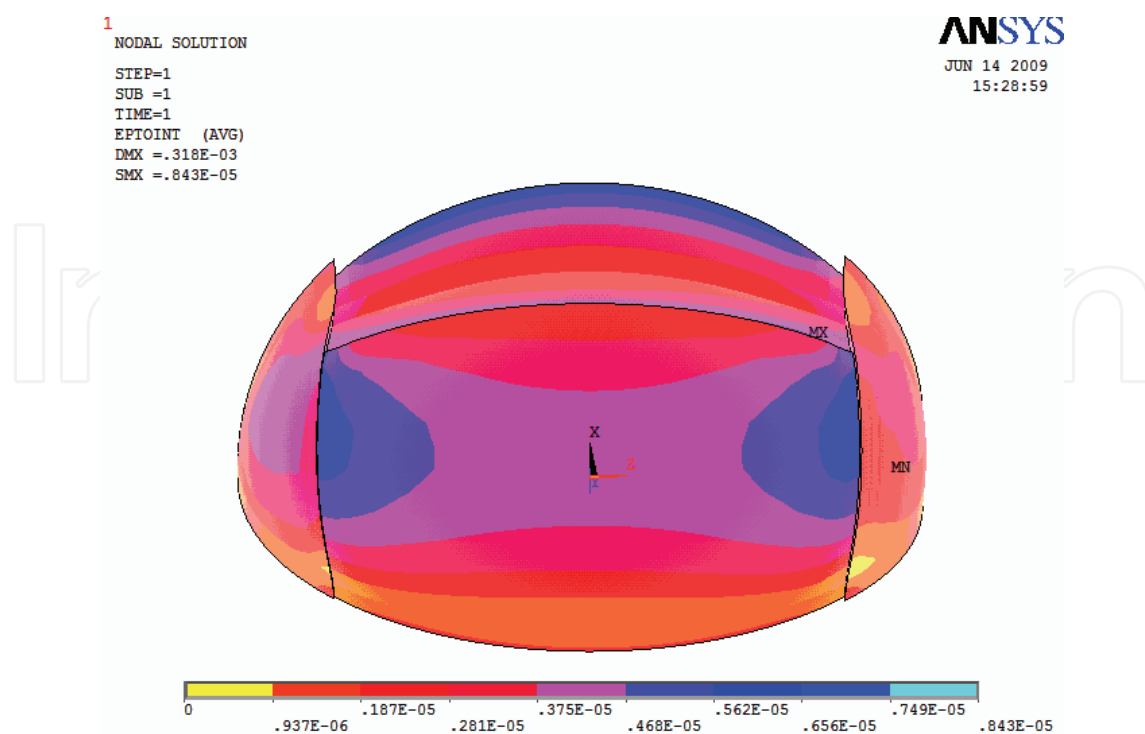


Fig. 3.7 Strain graph with hypothermia treatment when the ICP is 5.0kPa

ICP variation	Strains of 39.5°C	Strains of 33.5°C
kPa	$\mu\epsilon$	$\mu\epsilon$
2.0	1.510	1.500
2.5	1.880	1.870
3.0	2.260	2.250
3.5	2.630	2.620
4.0	3.010	2.990
4.5	3.390	3.370
5.0	3.760	3.740
6.0	4.520	4.490

Table 4. Strain data of cranial cavity simulated by ANSYS with the ICP variation

4. Results and Discussion

4.1 Results

This paper carries respectively on the stress and strain analysis on both conditions of ignoring and considering the viscoelasticity of human skull and duramater by finite-element software MSC_PPATRAN/NASTRAN and ANSYS as ICP changing from 1.5kPa to 5kPa. The three-dimensional finite element model of cranial cavity and the viscoelastic models of human skull and duramater are constructed in this paper. At the same time, the ANSYS finite-element software is in this paper used to reconstruct the three-dimensional cranial cavity of human being with the mild hypothermia treatment. The conclusion is as follows:

(1) The human skull and duramater are deformed as ICP changing, which is corresponding with mechanical deformation mechanism.

(2) When analyzing the strain of human skull and duramater as ICP changing by the finite-element software ANSYS, the strain of considering the viscoelasticity is about 14% less than that of ignoring the viscoelasticity of human skull and duramater. Because the viscoelasticity analysis by finite-element software ANSYS is relatively complex and the operation needs the huge memory and floppy disk space of computer, it is totally feasible to ignore the viscoelasticity while calculating the FEA strain of human skull and duramater as ICP changing.

(3) The viscosity plays an important role in the total deformation strain of human skull and duramater as ICP changing. In the strains analysis of human skull and duramater with the changing ICP by the finite-element software ANSYS, the viscous strain accounts for about 40% of total strain, and the elastic strain is about 60% of total strain.

(4) Because the strains of human skull are proportional to ICP variation and the caniocerebra characteristic symptoms completely correspond to different deformation strains of human skull, ICP can be completely obtained by measuring the deformation strains of human skull.

That is to say, the minitraumatic method of ICP by strain electrometric technique is feasible. Furthermore, ICP variation is respectively about 2.5kPa when the strain value of human skull is about $1.4\mu\epsilon$, about 3.5kPa when the strain value of human skull is about $2.1\mu\epsilon$, and about 5kPa when the strain value of human skull is about $3.9\mu\epsilon$.

(5) The strains decreased under the mild hypothermia environment about 0.56% than those under the normal temperature conditions during the same circumstance of ICP changes.

(6) The deformation scope of human skull is theoretically from $1.50\mu\epsilon$ to $4.52\mu\epsilon$ as the ICP changing from 2.0kPa to 6.0kPa under the normal situation, and from $1.50\mu\epsilon$ to $4.49\mu\epsilon$ under the mild hypothermia environment. Accordingly, the strains of skull deformation for mild, moderate and severe head injuries are separately $1.87\mu\epsilon$, $2.62\mu\epsilon$ and $3.74\mu\epsilon$ or so corresponding to ICP of 2.5kPa, 3.5kPa and 5.0kPa.

4.2 Discussion

From the eighties, the scholars abroad paid more attention to the effect on the mild and moderate hypothermia for the brain protection after the ischemic and traumatic brain injury, temperature from 29°C to 36°C [32]. And now the mild hypothermia has gradually been applied to the treatments of cerebral injury and ischemia. After the introduction of mild hypothermia in clinic, the impact must be considered on the protective measures to the other protection or measurement mechanisms. The deformation of cranial cavity had been calculated with the changing ICP by the finite element method [48]. Considering the increased ICP can cause central heat, taking into account, thereby requiring cooling measures, the hypothermia treatment should be carried out, which has been another important means of treating the severe craniocerebral trauma in recent years. Since the strains decreased under the mild hypothermia environment about 0.56% than those under the normal temperature conditions during the same circumstance of ICP changes, the mild hypothermia has obvious impact on the deformation of cranial cavity. That is to say, the effect must be considered on the mild hypothermia to measurement data in clinic or medical experiments while measuring the deformation of cranial cavity under the mild hypothermia environment simultaneously.

In this paper, the finite-element simulation was carried out to analyze the deformation of cranial cavity. Many complex relationships and influencing factors lie in the actual deformation of cranial cavity with the changing ICP. Therefore, in order to obtain the accurate deformation tendency of cranial cavity, the precise simulation to the finite-element model and further experimental studies in vivo and clinic need to be carried on.

5. References

- [1] Kaitai Li, Aixiang Huang, Qinghuai Huang. The finite element method and its application. 1st Eds, Xian'an: Xian'an Jiaotong University Publisher, 1992: 1-3
- [2] Guoqing Liu, Qingdong Yang. The applicable course of ANSYS in the engineering. China Railway Publisher, 2003
- [3] Ross, C.T.F. The finite element method of structural mechanics. 1st Eds. People Jiaotong Publisher, 1991. 1: 23-50

- [4] Siyuan Cheng. The methodology of finite element method. *Chongqing University Journal (Social science)*, 2001, 7(4): 61-63
- [5] Yijin Wang, Yongfeng Li, Kerong Dai, etc. Stress analysis on the femoral stem in the replacement of artificial joint. *Chinese Journal of Bone and Joint Injury* 1993; 8(1): 40
- [6] Meichao Zhang, Weidong Zhao, Lin Yua, Jiantie Li, Lei Tang, Shizhen Zhong. Three-dimensional reconstruction of the knee joint of digitized virtual Chinese male No.1 by finite element simulation. *Journal of First Military Medical University*, 2003, 23(6): 527-529
- [7] Chunbao Zhang, Xuanxiang Ma, Shaofeng Zhang, etc. Finite element analysis of the stress induced by an endodontic endosseous implant placed through a central incisor with periodontal compromises. *Journal of practical stomatology*, 2003, 19: 103
- [8] Jianchao Gui, Qiang Zhou, Xiangjie Gu, Haiqi Shen, Xin Ma, Jinsong Chen, Yijin Wang. Three dimensional finite element modeling study of the effect of femoral quality on hip arthroplasty. *The journal of bone joint injury*, 2000, 15(3): 212-240
- [9] Youxin Shu, Shuliang Xu, Riqi Chen, Xianxiang Liu. The study of the relation between the wrong using of pillow and the cause of cervical spondylosis with the spacial analytical method of finite element in dynamic models. *Journal of Traditional Medical Traumatology & Orthopedics*, 1999, 7(6): 9-12
- [10] Liyang Dai, Yinkan Xu, Wenming Zhang, Kaiyuan Tu, Peilai Cheng. A three-dimensional finite analysis of lumbar intervertebral disc. *Journal of Biomedical Engineering*, 1991, 8(3): 237-441
- [11] Meichao Zhang, Shizhen Zhong. The effects of transcription factor decoy on gene therapy. *Progress of anatomical sciences*, 2003, 9(1): 53-56
- [12] R. M. Jones. *Composite Material*. 1st Eds. Shanghai Science and Technology Publisher, 1981. 6: 41-73
- [13] Zhimin Zhang. *Structural Mechanics of Composite Material*. 1st Eds. Beijing: Publish of BUAA, 1993. 9: 85-86
- [14] Willinger, R., Kang, H.S., Diaw, B.M. Development and validation of a human head mechanical model. *Comptes Rendus de l'Academie des Sciences Series IIB Mechanics*, 1999, 327: 125-131.
- [15] Pithioux M, Lasaygues P, Chabrand P. An alternative ultrasonic method for measuring the elastic properties of cortical bone. *Journal of Biomechanics* 2002; 35: 961-968.
- [16] Hakim S, Watkin KL, Elahi MM, Lessard L. A new predictive ultrasound modality of cranial bone thickness. *IEEE Ultrason Sympos* 1997; 2: 1153-1156.
- [17] Hatanaka M. Epidural electrical stimulation of the motor cortex in patients with facial neuralgia. *Clinical Neurology and Neurosurgery* 1997; 99: 155.
- [18] Kabel J., Rietbergen van B., Dalstra M., Odgaard A., Huiskes R. The role of an elective isotropic tissue modulus in the elastic properties of cancellous bone. *Journal of Biomechanics* 1999; 32: 673-680.
- [19] J. Kabel, B. van Rietbergen, M. Dalstra, A. Odgaard, R. Huiskes, *Journal of Biomechanics*, 32 (1999) 673-680.
- [20] Noort van R., Black M.M., Martin T.R. A study of the uniaxial mechanical properties of human dura mater preserved in glycerol. *Biomaterials* 1981; 2: 41-45.
- [21] Kuchiwaki H., Inao S., Ishii N., Ogura Y., Sakuma N. Changes in dural thickness reflect changes in intracranial pressure in dogs. *Neuroscience Letters* 1995; 198: 68-70.

- [22] Pithioux M., Lasaygues P., Chabrand P. An alternative ultrasonic method for measuring the elastic properties of cortical bone. *Journal of Biomechanics* 2002; 35: 961-968.
- [23] Wood J.L. Dynamic response of human cranial bone. *Journal of Biomechanics* 1971; 4: 1-12.
- [24] Hilton G. Cerebral oxygenation in the traumatically brain-injured patient: are ICP and CPP enough? *The Journal of Neuroscience Nursing*, 2000; 32: 278-282.
- [25] Wu G.R., Zhang, Y.R., Wang, Y.Q., You, G.X. Changes of Intracranial Pressure during Head Impact in Monkeys and Protection of Head Impact Injuries (Chinese). *Acta Aeronautica et Astronautica Sinica (Sup)* 1999; 20: 54-56.
- [26] Willinger R., Kang H.S., Diaw B.M. Development and validation of a human head mechanical model. *Comptes Rendus de l'Academie des Sciences Series IIB Mechanics* 1999 ; 327: 125-131.
- [27] Cattaneo P.M., Kofod T., Dalstra M., Melsen B. Using the finite element method to model the biomechanics of the asymmetric mandible before, during and after skeletal correction by distraction osteogenesis. *Computer Methods in Biomechanics & Biomedical Engineering* 2005; 8(3): 157-165.
- [28] Amit G., Nurit G., Qiliang Z., Ramesh R., Margulies S.S. Age-dependent changes in material properties of the brain and braincase of the rat. *Journal of Neurotrauma* 2003; 20(11): 1163-1177.
- [29] Andrus C. Dynamic observation and nursing of ICP. *Foreign Medical Sciences (Nursing Foreign Medical Science)* 1992; 11(6): 247-249.
- [30] Min W. Observation and nursing for fever caused by Acute Cerebrovascular Disease. *Contemporary Medicine* 2008; 143: 100-101.
- [31] Shiozaki T., Sugimoto H., Taneda M., et al. Selection of Severely Head Injured Patients for Mild Hypothermia Therapy. *Journal of Neurosurgery* 1998; 89: 206–211.
- [32] Lingjuan C. Current situation and development trend at home and abroad of Hypothermia Therapy Nursing. *Chinese Medicine of Factory and Mine* 2005; 18(3): 268-269.
- [33] Yue X.F., Wang L., Zhou F. Experimental Study on the strains of skull in rats with the changing Intracranial Pressure. *Tianjin Medicine Journal*, 2007, 35(2): 140-141.
- [34] Yue X.F., Wang L., Zhou F. Strain Analysis on the Superficial Surface of Skull as Intracranial Pressure Changing. *Journal of University of Science and Technology Beijing*, 2006, 28(12) : 1143-1151.
- [35] Qiang X., Jianuo Z. Impact biomechanics researches and finite element simulation for human head and neck. *Journal of Clinical Rehabilitative Tissue Engineering Research*, 2008, 12(48) : 9557-9560.
- [36] Zong Z., Lee H., Lu C. A three-dimensional human head finite element model and power in human head subject to impact. *Journal of Biomechanics*, 2006, 39(2): 284-292.
- [37] Ren L., Hao L., Shuyuan L., et al. A study of the volume of cranial cavity calculating from the dimension of cranial outer surface in X-ray films—its stepwise regressive equation and evaluation. *Acta Anthropological Sinica*, 1999, 18(1): 17-21.
- [38] Yunhong L. Yanbo G. Yunjian W., et al. Experiment study on shock resistance of skull bone. *Medical Journal of the Chinese People's Armed Police Forces*, 1998, 9(7): 408-409.

- [39] Haiyan L., Shijie R., Xiang P., et al. The thickness measurement of alive human skull based on CT image. *Journal of Biomedical Engineering*, 2007, 24(5): 964-968.
- [40] Zhou L.F., Song D.L., Ding Z.R. Biomechanical study of human dura and substitutes. *Chinese Medical Journal*, 2002, 115(11): 1657-1659.
- [41] Willinger R., Kang H.S., Diaw B.M. Development and validation of a human head mechanical model. *Comptes Rendus de l'Academie des Sciences Series IIB Mechanics*, 1999, 327:125-131.
- [42] Odgaard A., Linde F. The Underestimation of young's modulus in compressive testing of cancellous bone specimens. *Journal of Biomechanics*, 1991, 24, 691-698.
- [43] Wenjun S., Jialin H. *Handbook of critical illness care*. People's Military Medical Press, 1994:75-77.
- [44] Dashi Z. The development and present status of mild hypothermia in cerebral protection[J]. *Moden Journal Neurosurg*, 2002, 2 (3): 133-135.
- [45] Bin W. Hong L. Investigation on the hypothermia treatment time course to the severe traumatic brain injury. *Chinese Journal of Clinical Neurosurgery*, 2008, 13(10): 628-629.
- [46] Joji Inamasu, Kiyoshi Ichikizaki. Mild hypothermia in neurologic emergency: an update. *Hypothermia in a Neurologic Emergency*, 2002, 40(2): 220-230.
- [47] Cuihua Z. Hui R. Study status of cooling methods to induce mild hypothermia. *Chinese Journal of Nursing*, 2006, 41(2): 170-172.
- [48] Yue X.F., Wang L., Zhou F. Finite element analysis on strains of viscoelastic human skull and duramater. *Journal of Basic Science and Engineering*, 2008, 16 (5): 686-694.

IntechOpen



Finite Element Analysis

Edited by David Moratal

ISBN 978-953-307-123-7

Hard cover, 688 pages

Publisher Sciyo

Published online 17, August, 2010

Published in print edition August, 2010

Finite element analysis is an engineering method for the numerical analysis of complex structures. This book provides a bird's eye view on this very broad matter through 27 original and innovative research studies exhibiting various investigation directions. Through its chapters the reader will have access to works related to Biomedical Engineering, Materials Engineering, Process Analysis and Civil Engineering. The text is addressed not only to researchers, but also to professional engineers, engineering lecturers and students seeking to gain a better understanding of where Finite Element Analysis stands today.

How to reference

In order to correctly reference this scholarly work, feel free to copy and paste the following:

Xianfang Yue (2010). Finite Element Analysis on Strains of Viscoelastic Human Skull and Duramater, Finite Element Analysis, David Moratal (Ed.), ISBN: 978-953-307-123-7, InTech, Available from: <http://www.intechopen.com/books/finite-element-analysis/finite-element-analysis-on-strains-of-viscoelastic-human-skull-and-duramater>

INTECH
open science | open minds

InTech Europe

University Campus STeP Ri
Slavka Krautzeka 83/A
51000 Rijeka, Croatia
Phone: +385 (51) 770 447
Fax: +385 (51) 686 166
www.intechopen.com

InTech China

Unit 405, Office Block, Hotel Equatorial Shanghai
No.65, Yan An Road (West), Shanghai, 200040, China
中国上海市延安西路65号上海国际贵都大饭店办公楼405单元
Phone: +86-21-62489820
Fax: +86-21-62489821

© 2010 The Author(s). Licensee IntechOpen. This chapter is distributed under the terms of the [Creative Commons Attribution-NonCommercial-ShareAlike-3.0 License](#), which permits use, distribution and reproduction for non-commercial purposes, provided the original is properly cited and derivative works building on this content are distributed under the same license.

IntechOpen

IntechOpen